Title

Modeling the Translocation and Transformation of Chemicals in the Soil-Plant Continuum: A Dynamic Plant Uptake Module for the HYDRUS Model

Journal

Water Resources Research, 55(11)

ISSN

0043-1397

Authors

Brunetti, Giuseppe
Kodešová, Radka
Šimůnek, Jiří

Publication Date

2019-11-01

DOI

10.1029/2019wr025432

Peer reviewed

Water Resources Research

RESEARCH ARTICLE
10.1029/2019WR025432

Modeling the Translocation and Transformation of Chemicals in the Soil-Plant Continuum: A Dynamic Plant Uptake Module for the HYDRUS Model

Giuseppe Brunetti[1], **Radka Kodešová**[2], **and Jiří Šimůnek**[3]

[1]Institute of Hydraulics and Rural Water Management, University of Natural Resources and Life Sciences, Vienna, Austria, [2]Faculty of Agrobiology, Food and Natural Resources, Department of Soil Science and Soil Protection, Czech University of Life Sciences Prague, Prague, Czech Republic, [3]Department of Environmental Sciences, University of California, Riverside, CA, USA

Key Points:
- A dynamic plant uptake module is coupled with the HYDRUS model to simulate the translocation of chemicals in the soil-plant continuum
- Theoretical and experimental scenarios are used to validate the coupled model and demonstrate its flexibility
- The model satisfactorily reproduces the measured carbamazepine translocation and transformation in three vegetables

Correspondence to:
G. Brunetti,
giuseppe.brunetti@boku.ac.at

Citation:
Brunetti, G., Kodešová, R., & Šimůnek, J. (2019). Modeling the translocation and transformation of chemicals in the soil-plant continuum: A dynamic plant uptake module for the hydrus model. *Water Resources Research*, *55*. https://doi.org/10.1029/2019WR025432

Received 25 APR 2019
Accepted 9 SEP 2019
Accepted article online 15 SEP 2019

Abstract Food contamination is responsible for thousands of deaths worldwide every year. Plants represent the most common pathway for chemicals into the human and animal *food chain*. Although existing dynamic plant uptake models for chemicals are crucial for the development of reliable mitigation strategies for food pollution, they nevertheless simplify the description of physicochemical processes in soil and plants, mass transfer processes between soil and plants and in plants, and transformation in plants. To fill this scientific gap, we couple a widely used hydrological model (HYDRUS) with a multicompartment dynamic plant uptake model, which accounts for differentiated multiple metabolization pathways in plant's tissues. The developed model is validated first theoretically and then experimentally against measured data from an experiment on the translocation and transformation of carbamazepine in three vegetables. The analysis is further enriched by performing a global sensitivity analysis on the soil-plant model to identify factors driving the compound's accumulation in plants' shoots, as well as to elucidate the role and the importance of soil hydraulic properties on the plant uptake process. Results of the multilevel numerical analysis emphasize the model's flexibility and demonstrate its ability to accurately reproduce physicochemical processes involved in the dynamic plant uptake of chemicals from contaminated soils.

1. Introduction

Food contamination is a direct consequence of environmental pollution and represents a major risk for human health. Recently, the Food and Agricultural Organization of the United Nations (Food and Agricultural Organization, 2019) reported that food-contaminated natural toxins or chemicals are responsible for more than 339,000 people falling ill and 20,000 dying worldwide every year. Plants represent the most common pathway into the human and animal *food chain* for environmental contaminants. Chemicals from polluted environments are uptaken by plants, where they are bioaccumulated and eventually metabolized in active by-products (e.g., Mattina et al., 2003; Sabourin et al., 2012; Zhang et al., 2009), some of which can be dangerous for human health (e.g., Kodešová et al., 2019a; Malchi et al., 2014; So et al., 1994; Warner et al., 1992). Thus, widespread pollution forces the scientific community to better understand physicochemical processes within the soil-plant-atmosphere continuum in order to develop reliable mitigation strategies for food risk assessment and food safety.

Numerical models certainly play a crucial role in reaching this goal. Several plant uptake models have been developed and tested in the past, ranging from empirical to mechanistic models. Topp et al. (1986) and Travis and Arms (1988) proposed two different empirical models correlating the concentration of a chemical compound in the plant's tissues with its physicochemical properties. Despite the advantages of simple analytical relationships, these models provide a rather coarse description of the plant uptake processes. Alternatively, Ryan et al. (1988) developed a semimechanistic screening model for assessing the uptake of nonionic chemicals from soil. However, due to its theoretical limitations (e.g., neglecting plant-air exchange, metabolism, and growth dilution), this model was only intended to provide a simple approach for *screening* chemicals for which plant uptake may be an important pathway for human exposure. Hung and Mackay (1997) proposed a classic mechanistic approach instead, describing the kinetics of uptake in leaves, stem, and roots

using a dynamic multicompartment model, which included xylem and phloem flows, gaseous exchange, growth dilution, and metabolization.

Similarly, Trapp (2007) and Rein et al. (2011) developed a mechanistic multicompartment model encompassing all major physicochemical processes happening during the dynamic plant uptake (DPU) process. The model, initially developed for neutral compounds, was later extended to ionic chemicals and tested successfully against measured data under different operating conditions (Trapp, 2009). Hurtado et al. (2016) used the DPU model to inversely estimate kinetic parameters from a greenhouse experiment on dynamic uptake of emerging contaminants in lettuce. In another study, Trapp (2015) successfully calibrated the DPU model to simulate uptake of chlorinated organic compounds in radish.

Despite acceptable results, existing DPU models generally lack an accurate description of physicochemical processes in soils, which are among the most important sources of pollution for plants (Eugenio et al., 2018). The variably saturated hydraulic behavior of the root zone and biogeochemical processes in the near-surface environment, such as solute sorption and degradation, strongly affect actual transpiration patterns and solute uptake across the root surfaces. The accurate numerical description of these processes is thus crucial for the development of reliable soil-plant models. Along these lines, Legind et al. (2012) and Trapp and Eggen (2013) coupled the multicompartment model of Trapp (2007) with a model of water and solute transport in soil based on the "tipping buckets" approach. Such a numerical approach usually assumes that, due to gravity, water can only percolate downwards as Darcian flow (e.g., Schroeder et al., 1994) and simplifies upward flow due to capillarity. Additionally, this approach requires several threshold values as input, including field capacity and wilting point, that are often poorly defined (Twarakavi et al., 2009). In particular, the physical meaning of field capacity is ambiguous (Twarakavi et al., 2009) and should be adjusted to site-specific conditions, considering its high impact on simulated transport processes.

Due to these theoretical limitations (Emerman, 1995; Scanlon et al., 2003), this approach is mostly suited for specific working conditions in which water flow is mainly driven by gravity (i.e., irrigated agriculture with predominantly downward vertical flow) and is not well suited for many other important environments in which capillarity plays an important role (e.g., rainfed agriculture and/or upward flow from shallow groundwater). This approach is often used when water flow in soils is a secondary process in the model, which instead focuses on providing a detailed description of a different primary process (e.g., crop growth [Boote et al., 2008; Shelia et al., 2018] and DPU of chemicals [Trapp, 2007], etc.). Its application in traditional modeling scenarios (i.e., uptake of chemicals from contaminated soils under transient atmospheric conditions) may thus result in poor model generalizability stemming from the theoretical model's inadequacy. On the other hand, hydrological models provide sophisticated hydraulic and hydrologic descriptions while simplifying other model components. Therefore, research efforts should focus on the development of integrated soil-plant models which include a more coherent description of physicochemical processes in both soil and plant domains (Vereecken et al., 2016).

Numerical models from vadose zone hydrology, which have been used extensively in the last decades (Jarvis & Larsbo, 2012; Šimůnek et al., 2016), offer great opportunities to head in this direction. In particular, Richards-based approaches have been used successfully in many applications and scientific fields (e.g., Brunetti et al., 2017, 2019; Brunetti, Porti, & Piro, 2018; Brunetti, Šimůnek, & Bautista, 2018; Cheyns et al., 2010, Hanson et al., 2006, Jellali et al., 2016, Scanlon et al., 2003). Nolan et al. (2005) compared the performance of the Richards-based and tipping bucket models in reproducing measured breakthrough curves of bromide and atrazine from two experimental facilities in Merced, California, and White River Basin, Indiana, respectively. Results of this study indicated a better accuracy of the Richards-based models (i.e., HYDRUS-2D, LEACHP, RZWQM, and VS2DT) than the tipping-bucket models (i.e., CALF, GLEAMS, and PRZM). Furthermore, the authors reported a numerical influence of grid cell thickness on the effective solute dispersivity in some tipping bucket models. In another study, Herbst et al. (2005) concluded that the Richards' equation-based models should perform better than the capacity-based approaches in terms of predicting soil moisture contents, drainage amounts, and actual evapotranspiration. Similar conclusions were also obtained in the model intercomparison study by Scanlon, Christman, et al. (2003).

Besides simplifying soil processes, it must be emphasized that existing DPU models also simplify metabolization chains in the plant's tissues. The *green liver* behavior of plants (Sandermann, 1994) is generally accounted for using a single first-order decay coefficient that summarizes enzymatic biodegradation of

compounds in the plant. Although obtaining comprehensive measurements of metabolites may be very difficult, such an approach strongly reduces the model flexibility due to its inability to describe the generation of metabolites usually encountered in actual conditions (Kodešová et al., 2019b). On the other hand, the use of parent-metabolites data is becoming more popular in other scientific fields, such as pharmacokinetic modeling (Bertrand et al., 2011; Stroh et al., 2013), that share some theoretical and practical similarities with the DPU models. Such joint parent-metabolites pharmacokinetics models are used to simulate transformation and interaction effects and can be used in conjunction with other numerical techniques (e.g., Dumont et al., 2013) to increase the model predictive capability. This emphasizes the need to further refine the numerical description of degradation chains in plants.

We aim to fill the aforementioned scientific gaps by developing a fully coupled soil-plant model capable of providing a mechanistic comprehensive description of transport and reaction processes in the soil-plant continuum. To this end, we couple the widely used hydrological model, HYDRUS (Šimůnek et al., 2016), with a modified version of the multicompartment DPU model proposed by Trapp (2007), that now accounts for differentiated multiple metabolization pathways in plant's tissues. HYDRUS is a Richards equation-based model that has been chosen due to its reliability, versatility, success in several model intercomparison studies (e.g., Nolan et al., 2005; Scanlon, Christman, et al., 2003), and widespread use among hydrologists (Šimůnek et al., 2016). The problem is addressed in the following way. First, theoretical background to numerically combine the soil and plant models is developed. Then, the modified DPU model is theoretically validated against the original implementation of Trapp (2007) and internally coupled with the HYDRUS code to minimize the computational cost. Finally, the developed soil-plant model is validated against measured data from an experiment on the translocation and transformation of carbamazepine (CBZ) in three types of vegetables. The analysis is further enriched by performing a global sensitivity analysis on the soil-plant model to identify factors driving the compound's accumulation in plants' shoots, as well as to clarify the role and importance of soil hydraulic properties on the plant uptake process.

2. Materials and Methods

2.1. An Integrated Soil-Plant Modeling Environment

To describe the fate of neutral compounds in the soil-plant system (Figure 1), we couple a widely used hydrological model (HYDRUS) with a multicompartment DPU model. While HYDRUS (Šimůnek et al., 2016) is a finite-element model for simulating the movement of water, heat, and multiple solutes in variably saturated porous media, the DPU model accounts for the movement of water and solutes through the plant while also accounting for differentiated multiple metabolization pathways in plant's tissues. Additionally, the HYDRUS model has a relatively sophisticated root water and nutrient uptake model (Šimůnek & Hopmans, 2009), which provides a link between HYDRUS and DPU. Figure 1 summarizes the physicochemical processes in the soil-plant continuum and their theoretical conceptualization in the coupled soil-plant model.

2.2. DPU of Neutral Compounds

In this section, we provide an overall description of the model structure and a theoretical background for physical and biogeochemical processes implemented in the DPU model.

2.2.1. Model Structure

The numerical model is based on the multicompartmental approach proposed by Trapp (2007) and further developed by Rein et al. (2011) and Legind et al. (2011). The model simulates the translocation and biodegradation of N neutral compounds in plants, which are conceptualized in four compartments: roots, stem, leaves, and fruits. The choice to focus only on neutral compounds is intended to be only a first step in the model development. Transport processes consist of advection (with xylem flow) and diffusive losses or gains, while reaction processes mainly represent the enzymatic biodegradation in plant's tissue. More specifically, the following processes are considered in the DPU model:

- *Translocation* of compounds from the roots to the stem and from the stem to leaves and fruits with the transpiration stream. The phloem flux is neglected.
- *Volatilization* of compounds in the stem, leaves, and fruits.
- *Gaseous and particle deposition* from air to the stem, leaves, and fruits.

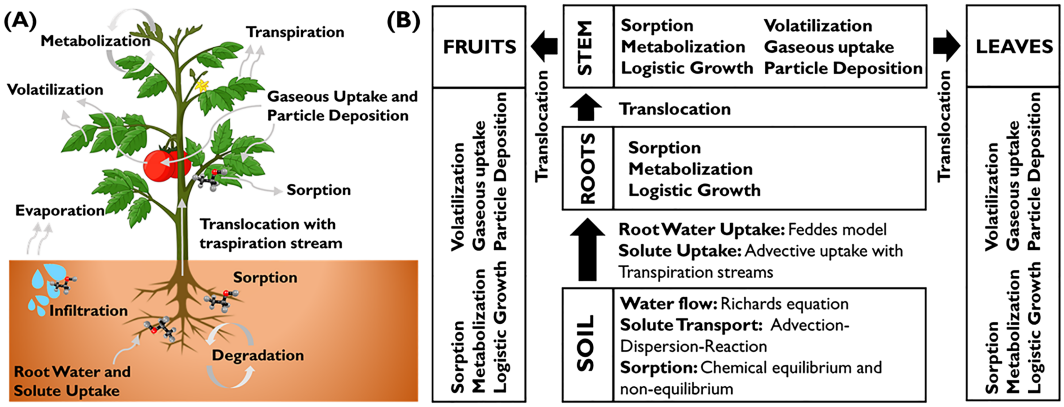

Figure 1. A schematic of the physicochemical processes in the (a) soil-plant continuum and their theoretical conceptualization in the (b) coupled soil-plant model.

- Compounds dilution by *plant growth* in all compartments.
- Compounds *metabolization* in all compartments.

The DPU model calculates the compounds' concentration in each compartment. The concentration matrix $\mathbf{C}$ has N rows (for each compound, represented below by a subscript i) and four columns (for each compartment, i.e., 1 = roots, 2 = stem, 3 = leaves, and 4 = fruits, represented below by a subscript j) and contains concentrations expressed as mass of each compound per fresh weight in different plants' compartments (M_s/M_{fw}, where subscript s refers to solutes and fw to fresh weight).

Transport and reaction processes depend on physical and chemical properties of the plant and compounds, respectively. In particular, the characteristics of four plant tissues are summarized in seven vectors.

$$\mathbf{W}=\begin{Bmatrix}W_1\\W_2\\W_3\\W_4\end{Bmatrix};\mathbf{L}=\begin{Bmatrix}L_1\\L_2\\L_3\\L_4\end{Bmatrix};\mathbf{M}^0=\begin{Bmatrix}M_1^0\\M_2^0\\M_3^0\\M_4^0\end{Bmatrix};\mathbf{M}^{\max}=\begin{Bmatrix}M_1^{\max}\\M_2^{\max}\\M_3^{\max}\\M_4^{\max}\end{Bmatrix};\mathbf{K}^{gr}=\begin{Bmatrix}K_1^{\mathrm{gr}}\\K_2^{\mathrm{gr}}\\K_3^{\mathrm{gr}}\\K_4^{\mathrm{gr}}\end{Bmatrix};\mathbf{S}^A=\begin{Bmatrix}S_1^A\\S_2^A\\S_3^A\\S_4^A\end{Bmatrix};\boldsymbol{\rho}=\begin{Bmatrix}\rho_1\\\rho_2\\\rho_3\\\rho_4\end{Bmatrix}, \quad (1)$$

where $\mathbf{W}$ is the water content of the plant (L^3/M_{fw}), $\mathbf{L}$ is the lipid content of the plant (M_l/M_{fw}, where subscript l refers to the lipid content), $\mathbf{M}_0$ is the initial plant mass (M_{fw}), $\mathbf{M}_{max}$ is the maximum plant mass (M_{fw}), $\mathbf{K}_{gr}$ is the growth rate coefficient (T^{-1}), $\mathbf{S}_A$ is the plant's specific area ($L^2M_{fw}{}^{-1}$), and $\boldsymbol{\rho}$ is the plant's density (M_{fw}/L^3). On the other hand, compounds' properties are described by four vectors.

$$\mathbf{K}_{\mathrm{OW}}=\begin{Bmatrix}\log K_{\mathrm{OW}_1}\\\log K_{\mathrm{OW}_2}\\\vdots\\\log K_{\mathrm{OW}_N}\end{Bmatrix};\mathbf{K}_{\mathrm{AW}}=\begin{Bmatrix}K_{\mathrm{AW}_1}\\K_{\mathrm{AW}_2}\\\vdots\\K_{\mathrm{AW}_N}\end{Bmatrix};\mathbf{C}_A=\begin{Bmatrix}C_{A_1}\\C_{A_2}\\\vdots\\C_{A_N}\end{Bmatrix};\mathbf{m}=\begin{Bmatrix}m^1\\m^2\\\vdots\\m^N\end{Bmatrix}, \quad (2)$$

where $\mathbf{K}_{OW}$ is the n-octanol-water partition coefficient (−), $\mathbf{K}_{AW}$ is the air-water partition coefficient (L^3/L^3), $\mathbf{C}_A$ is the compound concentration in the air (M_s/L^3), and $\mathbf{m}$ is the molar mass (M). Other required inputs are the air temperature T (K) and the relative humidity ϕ (−).

2.2.2. Mass Balance

The mass balance of N compounds in the four plant's compartments is mathematically described using a system of ordinary differential equations that is written in a compact form as

$$\frac{d\mathbf{C}}{dt}=\mathbf{Q}_{\mathrm{IN}}+\mathbf{Q}_{\mathrm{DEP}}+\mathbf{Q}_{\mathrm{GAS}}-\mathbf{Q}_{\mathrm{TR}}-\mathbf{Q}_{\mathrm{VOL}}+\boldsymbol{\Omega}, \quad (3)$$

where $\mathbf{Q}_{IN}$ is the inflow flux ($M_s{\cdot}M_{fw}{}^{-1}{\cdot}T^{-1}$; for each compound and each compartment), $\mathbf{Q}_{DEP}$ is the deposition of a chemical from particle deposition, $\mathbf{Q}_{GAS}$ is chemical gaseous uptake from the air, $\mathbf{Q}_{TR}$ is the translocation flux between compartments, $\mathbf{Q}_{VOL}$ is the volatilization flux, and $\boldsymbol{\Omega}$ represents reactions.

In the numerical model, equation (3) is solved implicitly in time using the backward Euler method (Butcher, 2016) to increase the stability of the numerical solution.

$$\frac{\mathbf{C}_{t+\Delta t}-\mathbf{C}_t}{\Delta t} = \mathbf{Q}_{\mathrm{IN}}^{t+\Delta t} + \mathbf{Q}_{\mathrm{DEP}}^{t+\Delta t} + \mathbf{Q}_{\mathrm{GAS}}^{t+\Delta t} - \mathbf{Q}_{\mathrm{TR}}^{t+\Delta t} - \mathbf{Q}_{\mathrm{VOL}}^{t+\Delta t} + \mathbf{\Omega}^{t+\Delta t}. \tag{4}$$

Equation (4) is expressed as a linear equation system, which is solved using the iterative quasi-Newton Broyden's method (Broyden, 1969) at each time step.

2.2.3. Plant Growth

Many annual crops exhibit a logistic growth characterized by an exponential growth at the beginning and an asymptotic behavior towards ripening. Accordingly, the change of the plant mass in each compartment $\mathbf{M}$ ($\mathrm{M_{fw}}$) as a function of time t (T) is expressed as

$$\frac{d\mathbf{M}}{dt} = \mathbf{K}_{\mathrm{gr}}\mathbf{M}\left(1-\frac{\mathbf{M}}{\mathbf{M}_{\max}}\right). \tag{5}$$

The plant mass in each compartment can be calculated by integrating the logistic growth function as follows:

$$\mathbf{M}(t) = \frac{\mathbf{M}_{\max}}{1+\left(\frac{\mathbf{M}_{\max}}{\mathbf{M}_0}-1\right)\exp^{-\mathbf{K}_{\mathrm{gr}}t}}. \tag{6}$$

The plant surface area $\mathbf{A}$ ($\mathrm{L^2}$) is related to the plant mass $\mathbf{M}$ through the specific surface area $\mathbf{S}_A$ ($\mathrm{L^2/M_{fw}}$).

$$\mathrm{A}_j(t) = S_j^A M_j(t) \tag{7}$$

where index j refers to four plant compartments. The model can alternatively use measured plant growth data and interpolate between measured data points.

2.2.4. Chemical Equilibrium and Partitioning

The typical time scale for chemical diffusion of neutral compounds through a cell membrane is negligible compared to the time scale of soil-plant processes. Under such circumstances, the rate of the sorption process is fast enough to consider instantaneous equilibrium, and the capacity of a chemical to diffuse across membranes can be described by the equilibrium partition coefficient. In particular, the equilibrium partitioning between a hydrophobic phase (lipids, oils, etc.) and water is described by the n-octanol-water partition coefficient K_{OW} (−). Measured values are available for many compounds, and they are usually expressed using a logarithmic scale. Similarly, the coefficient K_{AW} (−) describes the partitioning between liquid and air.

Briggs et al. (1982) defined a plant-water partition coefficient $\mathbf{K}_{\mathrm{PW}}$ ($\mathrm{L^3M_{fw}}^{-1}$), which is expressed in its matrix form as

$$\mathrm{K_{PW}}_{ij} = W_j + L_j a K_{\mathrm{OW}_i}^b \qquad i = 1, N \text{ and } j = 1, 4, \tag{8}$$

where W_j and L_j are the water ($\mathrm{L^3/M_{fw}}$) and lipid contents of the plant compartments ($\mathrm{M_l/M_{fw}}$), respectively, a is a coefficient ($\mathrm{L^3/M_l}$) usually assumed 0.00122 $\mathrm{m/kg_l}$ (Trapp, 2007), and b is an exponent equal to 0.77 and 0.95 for roots and plant shoots, respectively. Indices i and j refer to matrix columns (to N compounds) and rows (four compartments), respectively. It must be emphasized that the accuracy of equation (8) in predicting the sorption mechanism in the plant decreases with the polarity of the investigated chemical compound (Li et al., 2005). Therefore, for highly polar compounds, it is recommended to experimentally characterize the sorption mechanism.

2.2.5. Translocation

Most plants have two transport systems inside: xylem and phloem. Xylem is a nonliving vascular system that is hydraulically connected to phloem (Brodersen et al., 2019). Water is drawn upwards by physical forces. Phloem is composed of living cells, the sieve tubes. The flux in phloem generally occurs from the leaves to the fruits. In particular, phloem transports sugar and other essential substances. Xylem is responsible for the water translocation from the roots to other plant compartments induced by plant transpiration.

The effect of the plant water storage is neglected (e.g, Javaux et al., 2013; Manoli et al., 2014). Such assumption, which is valid only for small crops (Hartzell et al., 2017; Vogel et al., 2017), implies that the xylem flow $\mathbf{Q}_{XYL}$ (L^3/T) is equal to the transpiration stream through the roots and stem, Q_{TP}, while it is partitioned in fruits and leaves using corresponding surface areas (Trapp, 2007).

$$\mathbf{Q}_{XYL} = \left\{ Q_{TP} \;\; Q_{TP} \;\; Q_{TP} - \frac{A_4 Q_{TP}}{A_4 + A_3} \;\; \frac{A_4 Q_{TP}}{A_4 + A_3} \right\}. \tag{9}$$

The solute translocation flux $\mathbf{Q}_{TR}$ ($M_s \cdot M_{fw}{}^{-1} \cdot T^{-1}$) is expressed as

$$Q_{TR_{ij}} = \frac{Q_{XYL_{ij}} C_{ij}}{M_j K_{PW_{ij}}}. \tag{10}$$

Leaves and fruits are the end of the xylem system; and thus, no further translocation is assumed in these compartments. Such an assumption implies that to facilitate the model implementation, we can similarly define for each compartment the solute inflow $\mathbf{Q}_{IN}$ ($M_s \cdot M_{fw}{}^{-1} \cdot T^{-1}$), which contains the compounds. In particular, solute inflow into the root compartment is represented by actual solute uptake calculated by HYDRUS for a soil surface area of 1 m^2 divided by the roots mass ($M_s \cdot M_{fw}{}^{-1} \cdot T^{-1}$), while the translocation flux from the roots is the inflow for the stem. Finally, the xylem flow from the stem is divided into two streams that enter leaves and fruits.

2.2.6. Exchange Plant-Air: Plant Permeability

The plant-air exchange is regulated by the permeability of the plant's components (Trapp, 2007). A chemical in the air has to overcome only the air boundary layer between the leaf surface and the turbulent atmosphere. It can then adsorb on the leaf surface, which is a waxy layer known as the cuticle. On the other hand, a chemical transported by the transpiration stream into the leaf can be exchanged with air through cuticles or stomata. Thus, three different phases provide resistance (aqueous phase, lipid phase, and gas phase) and two pathways are in parallel (stomatal and cuticular pathways).

The more lipophilic a compound, the higher its permeability across the cuticle barrier.

$$P_{C_i} = 10^{0.704 \log K_{OW_i} - 11.2}, \tag{11}$$

where $\mathbf{P}_C$ is the cuticle conductance (L/T). The next resistance is provided by the air boundary layer surrounding the plant, $\mathbf{P}_{air}$ (L/T). Resistance of 200 s/m was estimated as typical for a chemical with molar weight $m = 300$ g/mol (Thompson, 1983). The conductance of the air boundary layer, $\mathbf{P}_{air}$, for a chemical with a molar mass m is thus

$$P_{air_i} = \frac{K_{AW_i} \sqrt{300}}{200 \sqrt{m_i}}, \tag{12}$$

where m is the molar mass of the chemical. However, water does need to cross the aqueous layer in the apoplast. The permeability of this layer $\mathbf{P}_{aqua}$ (L/T) is

$$P_{aqua_i} = D_{O_2} \sqrt{32 \Big/ \frac{m_i}{z,}} \tag{13}$$

where z is the thickness of the aqueous layer assumed 0.0005 m, and D_{O2} is the diffusion coefficient of oxygen in water (2×10^{-9} m^2/s). Thus, the total cuticle permeability $\mathbf{P}_{C,tot}$ (L/T) is

$$\mathbf{P}_{C,tot} = \frac{1}{\frac{1}{\mathbf{P}_C} + \frac{1}{\mathbf{P}_{air}} + \frac{1}{\mathbf{P}_{aqua}}}. \tag{14}$$

The role of the stomata is gas exchange. While the stomata are open, carbon dioxide is taken up, and water vapor is lost. Details on the calculation of transpiration are provided in the following sections. The conductance of the stomata, $\mathbf{P}_S$ (L/T), can thus be calculated from the xylem flow $\mathbf{Q}_{XYL}$ as

$$P_{S_{ij}} = \frac{Q_{\mathrm{XYL}_j}\rho_{\mathrm{water}}}{A_j\left(C_{\mathrm{H2O,sat}} - \phi C_{\mathrm{H2O,sat}}\right)}\frac{\sqrt{18}}{\sqrt{m_i}}K_{\mathrm{AW}_i}, \tag{15}$$

where ϕ is the relative air humidity (−), ρ_{water} is the water density (M/L^3), and $C_{\mathrm{H2O,sat}}$ is the water concentration inside plant's shoots (M/L^3), which can be calculated as

$$C_{\mathrm{H2O,sat}} = \frac{p_{\mathrm{H2O}}}{461.9T}, \tag{16}$$

where p_{H2O} is the saturation vapor pressure (ML^{-1}·T^{-2}) at a given temperature T (K), calculated using the empirical Magnus equation:

$$p_{\mathrm{H2O,sat}} = 610.7 \times 10^{\frac{7.5(T-273.15)}{237+(T-273.15)}}. \tag{17}$$

The exchange of the chemical through cuticle and stomata occurs in parallel, and thus, permeabilities are added to derive the total permeability for the exchange between the plant and air, $\mathbf{P}_P$ (L/T):

$$\mathbf{P}_P = \mathbf{P}_S + \mathbf{P}_{C,\mathrm{tot}}. \tag{18}$$

2.2.7. Volatilization

Chemicals can leave or enter the plant in several ways. This exchange process is regulated by the plant-air partition vector $\mathbf{K}_{\mathrm{PA}}$ (L3/L^3), which is expressed as

$$\mathrm{K}_{\mathrm{PA}_{ij}} = \frac{K_{\mathrm{PW}_{ij}}\rho_j}{K_{\mathrm{AW}_i}}. \tag{19}$$

No volatilization is assumed in the roots since they are generally not exposed to air. The volatilization rate depends on the permeability of plant's compartments, $\mathbf{P}_P$. In the developed model, only the cuticular pathway is used for the stem, while for fruits and leaves, exchanges of the chemical occur through the cuticle and stomata in parallel (Rein et al., 2011). The volatilization flux vector $\mathbf{Q}_{\mathrm{VOL}}$ ($\mathrm{M_s{\cdot}M_{fw}}^{-1}{\cdot}\mathrm{T}^{-1}$) is expressed as

$$Q_{\mathrm{VOL}_{ij}} = \frac{A_j P_{P,ij}\rho_j C_{ij}}{M_j K_{\mathrm{PA}_{ij}}}. \tag{20}$$

2.2.8. Gaseous Uptake and Particle Deposition

The gaseous uptake flux of chemicals from the air, $\mathbf{Q}_{\mathrm{GAS}}$ ($\mathrm{M_s{\cdot}M_{fw}}^{-1}{\cdot}\mathrm{T}^{-1}$), is defined as:

$$\mathrm{Q}_{\mathrm{GAS}_{ij}} = \frac{A_j P_{P,ij}\left(1-f_p\right)C_{A_i}}{M_j}, \tag{21}$$

where f_p is the fraction of a chemical adsorbed on the particles (−). The uptake of chemical from particle deposition, $\mathbf{Q}_{\mathrm{DEP}}$ ($\mathrm{M_s{\cdot}M_{fw}}^{-1}{\cdot}\mathrm{T}^{-1}$), is:

$$\mathrm{Q}_{\mathrm{DEP}_{ij}} = \frac{A_j v_{\mathrm{dep}} f_p C_{A_i}}{M_j}, \tag{22}$$

where v_{dep} (L/T) is the particle deposition velocity assumed 0.001 m/s (Trapp & Matthies, 1998).

2.2.9. Metabolization of Neutral Compounds

Plant compounds' metabolism is divided into three stages: transformation (I), conjugation (II), and compartmentation and storage processes (III), although plants have no excretion systems. Cellular storage sites are the vacuole and the cell wall (Sandermann, 1992). Plants thus have the ability to metabolize chemicals by exploiting the enzyme degradation. Furthermore, it is well known that millions of bacteria live on, but also inside of, plants. Most of these bacteria are heterotrophic and use chemicals as a substrate to grow. Compounds can be used as an electron acceptor, an electron donor, as an energy source, or as a precursor for other molecules. This opens opportunities—plants can be "vaccinated" with degrader bacteria to degrade pollutants (phytoremediation) or pesticides (Barac et al., 2004; Glick, 2010).

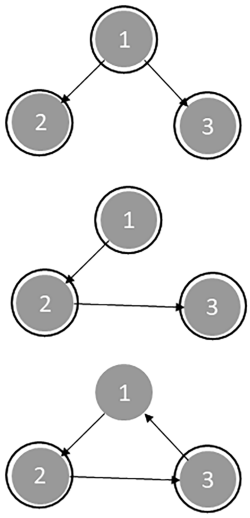

$$\mathbf{\Omega}_1 = \begin{Bmatrix} -\tau_{11}C_{11} + 0.0 + 0.0 \\ +\tau_{21}{}'C_{11} - \tau_{22}C_{21} + 0.0 \\ +\tau_{21}{}'C_{11} + 0.0 - \tau_{33}C_{31} \end{Bmatrix} \quad \textbf{(A) Double chain}$$

$$\mathbf{\Omega}_1 = \begin{Bmatrix} -\tau_{11}C_{11} + 0.0 + 0.0 \\ +\tau_{21}C_{11} - \tau_{22}C_{21} + 0.0 \\ 0.0 + \tau_{32}{}'C_{21} - \tau_{33}C_{31} \end{Bmatrix} \quad \textbf{(B) Sequential chain}$$

$$\mathbf{\Omega}_1 = \begin{Bmatrix} -\tau_{11}C_{11} + 0.0 + \tau_{13}{}'C_{31} \\ +\tau_{21}{}'C_{11} - \tau_{22}C_{21} + 0.0 \\ 0.0 + \tau_{32}{}'C_{21} - \tau_{33}C_{31} \end{Bmatrix} \quad \textbf{(C) Closed chain}$$

Figure 2. Examples of (a) double, (b)sequential, and (c) closed metabolization chains of three compounds in the *j*th compartment (in this case $j = 1$, i.e., in the roots). Black circles indicate an incomplete conversion of the reactant in by-products.

Nevertheless, traditional modeling approaches are based on the use of a single first-order rate coefficient to describe compound's biodegradation (e.g., Legind et al., 2011; Rein et al., 2011; Trapp, 2007). Such an approach completely neglects the transformation chain in the plant's tissues, which leads to the formation of new chemical by-products. For instance, CBZ can generate both hydroxylated and conjugated metabolites, which can be further degraded (Goldstein et al., 2018). Furthermore, not all compounds are generally degraded since plants have an upper limit on the compound compartmentation. These metabolites, which can be chemically active, are important for risk assessment (e.g., So et al., 1994; Warner et al., 1992) and must be considered in the analysis. In addition to that, recent studies have shown differentiated biodegradation rates in different plant's compartments (e.g., Fantke & Juraske, 2013; Kodešová et al., 2019b), suggesting the need to use a more flexible mathematical description. To overcome such limitations in the present model, the plant metabolization is modeled using multiple metabolization matrices $\mathbf{\Gamma}_j$. These matrices consist of multiple first-order rate coefficients, which provide connections between parent and daughter species. The matrix $\mathbf{\Gamma}_j$ is a square matrix of a dimension N (i.e., a number of metabolites considered).

$$\mathbf{\Gamma}_j = \begin{Bmatrix} -\tau_{11} & .. & +\tau'_{1N} \\ : & \cdot & : \\ +\tau'_{N1} & .. & -\tau_{NN} \end{Bmatrix} \text{ with } \sum_{i=1}^{N} \Gamma_{ij} \leq 0. \tag{23}$$

where τ are first-order rate constants for the compound (T^{-1}), while τ' are similar first-order rate constants providing connections between individual chain species (T^{-1}). The metabolization rate vector for the *j*th compartment, $\mathbf{\Omega}_j$ ($M_s \cdot M_{fw}{}^{-1} \cdot T^{-1}$), is thus defined as the dot product of the metabolization and concentration matrices.S

$$\mathbf{\Omega}_j = \mathbf{\Gamma}_j \cdot \mathbf{C}_j = \begin{Bmatrix} -\tau_{11} & .. & +\tau'_{1N} \\ : & \cdot & : \\ +\tau'_{N1} & .. & -\tau_{NN} \end{Bmatrix} \cdot \begin{Bmatrix} C_{1j} \\ : \\ C_{Nj} \end{Bmatrix}. \tag{24}$$

The proposed approach guarantees high modeling flexibility for handling multiple nonsequential degradation chains and simulating the effect of reaction yields. Figure 2 shows a schematic of three metabolization chains in the *j*th compartment with their respective model implementations.

2.3. Implementation in the HYDRUS Model

The compounds' translocation in the plant is mainly driven by actual transpiration and solute uptake fluxes, which are in turn dependent on the pressure head and solute distribution in the root zone (de Jong van Lier

et al., 2013), respectively. Huber et al. (2014) demonstrated that soil moisture heterogeneity strongly influences plant hydraulics. Hence, an accurate description of the physicochemical processes in the near-surface environment is crucial for developing a reliable soil-plant modeling tool (Vereecken et al., 2016). To this aim, the mechanistic model HYDRUS is coupled with the DPU model to further extend its modeling capabilities to the plant domain thus obtaining a fully integrated modeling environment for contaminant risk assessment. In this section, we first provide an overview of the HYDRUS model and then a thorough description of the coupling strategy and practical implementation of the coupled soil-plant-atmosphere model.

2.3.1. HYDRUS Model

HYDRUS (Šimůnek et al., 2016) is a finite-element model for simulating the movement of water, heat, and multiple solutes in variably saturated porous media. It numerically solves the Richards equation for multidimensional variably saturated water flow.

$$\frac{\partial \theta}{\partial t} = \nabla[K \cdot \nabla(h - z)] - S(h), \tag{25}$$

where t is time (T), z is the vertical coordinate (L), θ is the volumetric water content (L^3/L^3), K is the unsaturated hydraulic conductivity (L/T), h is the pressure head (L), and S is a sink term representing root water uptake (T^{-1}).

Solute transport can be simulated in the liquid, solid, and gaseous phases, though the latter is not of immediate interest in soil-plant modeling. Therefore, the transport of the ith solute in the soil is described using the advection-dispersion-reaction equation, assuming that solutes can exist only in the solid and liquid phases.

$$\frac{\partial \theta C_i}{\partial t} + \frac{\partial \rho s_i}{\partial t} = \nabla\left(\theta D_i^W \cdot \nabla C_i\right) - \nabla(qC_i) - r_{a,i} - \phi_i, \tag{26}$$

where C_i is the concentration of the ith solute in the liquid phase (M/L), s_i is the concentration of the ith solute in the solid phase (M/M), ρ is the soil density (M/L), D_i^W is the dispersion tensor for the ith solute in water (L^2/T), q is the water flux (L/T), r_a is the root solute uptake term ($M \cdot L^{-3} \cdot T^{-1}$), and ϕ_i represents the reaction sink/source term ($M \cdot L^{-3} \cdot T^{-1}$). Several equilibrium and nonequilibrium models are available to simulate solute sorption to the solid phase (Šimůnek et al., 2016), while zero-order or first-order coefficients are used to simulate reaction processes.

2.3.2. Root Water and Solute Uptake

Beer's equation is first used to partition reference evapotranspiration into potential transpiration, S_p, and potential soil evaporation, E_p (e. g., Ritchie, 1972). The Leaf Area Index (LAI) is needed to partition evaporation and transpiration fluxes. Equations (6) and (7) are used to calculate the mass and area of the leaves, respectively, with the latter then converted to LAI. For a detailed explanation of evapotranspiration partitioning in HYDRUS, please refer to Sutanto et al. (2012).

The actual transpiration stream, Q_{TP}, is calculated as the integral of actual root water uptake in the root zone domain, R:

$$Q_{\mathrm{TP}} = \int_R S(h,x,y,z)dxdydz = S_P \int_R a(h,x,y,z)b(x,y,z)dxdydz. \tag{27}$$

where $S(h,x,y,z)$ is actual root water uptake, $a(h,x,y,z)$ is a dimensionless water stress response function, and $b(x,y,z)$ is a root density distribution function. The stress response function a depends on the soil pressure head h and has a range of values between 0 and 1. It parametrizes the effects of the energy status of soil water caused by capillary, gravitational, and osmotic forces, as well as the oxygen deficit. Feddes et al. (1978) proposed a water stress response function in which water uptake is assumed to be zero close to soil saturation (P0) and for pressure heads higher (in absolute values) than the wilting point (P3). Water uptake is assumed to be optimal between two specific pressure heads (POpt, P2H, or P2L), which depend on the plant type. At high potential transpiration rates (5 mm/day in the model simulation), stomata start to close at lower pressure heads (P2H; in absolute value) than at low potential transpiration rates (1 mm/day; P2L). Parameters of the stress response function for a majority of agricultural crops can be found in various databases (e.g., Taylor & Ashcroft, 1972; Wesseling et al., 1991).

The root density function, $b(x,y,z)$, modulates actual root water uptake depending on the root growth and density. First, equation (6) is used to calculate the root growth, which is synchronized between HYDRUS and DPU models. Then, the equation proposed by Hoffman and van Genuchten (1983) is used to determine, at each time step, the root density and actual root water uptake at different soil locations. This numerical approach is applied to one-dimensional as well as multidimensional soil-roots modeling scenarios. No feedback mechanism between the plant and the soil domain is considered. In case of soil heterogeneities, the possibility to have a spatial description of soil processes increases the accuracy of the soil-plant model predictions (Huber et al., 2014) compared to more simplistic approaches that assume a homogeneous soil profile.

In the case of passive root solute uptake, r_a is equal to the product of the sink term S in the water flow equation (25) and the concentration of the sink term C_i (M/L^3). In the case of active root solute uptake, r_a is calculated using the plant nutrient demand (which is plant and time specific) and the solute distribution in the soil (Šimůnek & Hopmans, 2009). All compounds dissolved in water are taken up by plant roots when C_i is lower than a maximum allowed solution concentration $C_{\max}$ (M/L^3). Details about the implementation of root solute uptake in HYDRUS can be found in Šimůnek and Hopmans (2009).

2.3.3. Coupling Strategy and Implementation

Neutral compounds are generally passively taken up by plants with the transpiration flux. Under such conditions, the plant uptake process is considered purely advective. As reported by Rein et al. (2011), the error of approximating solute uptake by only advection is small and not relevant in practice. This is mathematically expressed as a *one-way* coupled system, in which the soil and plant domains are *sequentially* coupled and no feedback mechanism exists between the two domains. Briefly, HYDRUS calculates actual root water and solute uptake, which are then used as input for the roots compartment where the DPU starts.

The standard HYDRUS code has been modified to include the DPU component. In particular, all subroutines related to the DPU model have been collected in a separate FORTRAN file. This file contains reading and writing subroutines, as well as the solver for equation (4), which are called by the main code at each time step during model execution. It must be emphasized that the following coupling approach can be applied to one-dimensional soil profiles (i.e., HYDRUS-1D) as well as to multidimensional soil domains (i.e., HYDRUS-2D/3D). The practical implementation can be summarized in a few steps.

1. *Initialization*: The HYDRUS model is set up in the usual way by defining all simulated processes, domain properties, and input parameters. At the same time, an American Standard Code for Information Interchange file is used to collect plant physical characteristics (equation (1)), compounds' chemical properties (equation (2)), and metabolization matrices for each compartment (equation (24)). In this step, multiple HYDRUS and DPU output files are created. In particular, N (i.e., a number of compounds) files are initialized for the DPU model, each of which is used to store time series of simulated compounds' concentrations in each compartment.
2. *Coupled model execution*: The HYDRUS main code initializes variables, reads the input, and starts the calculation. At each time step, water flow and heat and solute transport are solved first. Simulated actual root water and solute uptakes are then area-averaged to unit area and passed to the DPU solver, which in turn calculates the compounds' distribution in plant's tissues. The time step is dictated by the main HYDRUS solver. Preliminary numerical tests were carried to assess this coupling approach and investigate the stiffness of the sink term in equation (25). Such tests considered compounds with different K_{OW} and K_{AW} under variable atmospheric conditions. Simulations remained numerically stable in all tests, thus, suggesting a relatively low stiffness of the DPU model.
3. *Output*: If the simulation is convergent, preinitialized output files are populated with results of the numerical simulation, which continues until the simulation period ends. Finally, mass-balance errors are calculated for both soil and plant domains.

2.4. Theoretical Validation

Before the proper experimental validation of the coupled soil-plant model, the DPU component has been validated against a Microsoft Excel® implementation of the DPU model proposed by Trapp (2007), which is available on his website (https://homepage.env.dtu.dk/stt/). Theoretical validation is a needed step when

Table 1
Input parameters used in the theoretical validation of the dynamic plant uptake model

Parameter	Roots	Shoots
W (cm^3/g_{fw})	0. 89	0. 85
L (g_l/g_{fw})	0.025	0.02
M (g_{fw})	1000	1000
S_A (cm^2/g_{fw})	0.0	50.0
τ_{11} (day^{-1})	0.15	0.15
Air		
C_A (g_s/cm^3)	1e-13	
f_p (−)	0.5	
v_{dep} (cm/day)	8640	
Compound		
log K_{OW} (−)	2.00	
K_{AW} (cm^3/cm^3)	0.00005	

testing and developing models since it avoids the influence of unpredictable sources of uncertainty of experimental data, which could mask inaccuracies in the model implementation.

2.4.1. Synthetic Scenario Description

The synthetic scenario considers the translocation of a contaminant in a perennial shrub conceptualized in two compartments (i.e., roots and shoots). The plant is exposed to contaminated soil water and air for a simulation period of 1,200 days. Two 1-day injection pulses of 0.01 g of the compound are used to load the system at Days 300 and 600. Gaseous uptake, particle deposition, and compound's volatilization are considered in the numerical simulation, while plant growth is neglected (i.e., a constant plant mass, **M**). Constant actual transpiration of 1,000 cm^3/day is assumed. The plant's permeability $\mathbf{P}_P$ is reduced to a scalar value, which is assumed to be constant and equal to 8,640 cm/day. The time series of simulated solute concentrations in different compartments is used to validate the DPU model. Plant's characteristics and input parameters are summarized in Table 1.

2.5. Experimental Validation

Measured data are taken from a recently published study by Kodešová et al. (2019b), which focused on the translocation and biodegradation of selected pharmaceuticals in different plants. In the present study, only measured data about dynamic uptake of CBZ and its main metabolites (i.e., 10,11-epoxide carbamazepine [EPX], and oxcarbazepine [OXC] in lamb's lettuce, spinach, and arugula) are used. The modeling study is further enriched by a global sensitivity analysis to identify the most important factors influencing the accumulation of CBZ in spinach shoots. The overall analysis aims to provide a preliminary assessment of the developed model against observed data and to demonstrate its flexibility and use potential. In the following sections, we provide a general overview of the experiment, modeling settings, and numerical methods used. For a thorough description of the experiment, please refer to Kodešová et al. (2019b).

2.5.1. Case Study Description

Experiments were carried out under greenhouse conditions, with average air temperature and humidity of 22 °C and 35%, respectively. A single plant was planted in a small pot in five replicates of each soil (three soils were used) and treatment, which consisted of an injection of a single compound or a mixture of three pharmaceuticals. In the present study, only data relative to an injection of a single compound in Haplic Chernozem soils are considered. The irrigation regime and injected concentrations are reported in Table 2. Each pot was perforated at the bottom and had a height of 5.5 cm and a surface area of 25 cm^2 and, additionally, was placed on top of a plastic plate that provided a limited accumulation of water during the experiment. The soil surface was covered with a thin layer of quartz-sand gravel to avoid cross-contamination of treated soil pots. An evaporation pan placed near the pots measured evaporation in the greenhouse, which was generally constant and approximately equal to 0.2 cm/day. A pan coefficient of 1.0 was assumed to estimate the reference evapotranspiration (Zeng et al., 2009).

Table 2
Irrigation doses for a single plant and concentrations of carbamazepine

	Irrigation (cm^3)		Carbamazepine
Day	Spinach/Arugula	Lamb's lettuce	[g/cm^3]
0		Sprout	
16	30.0	0.0	6.50e-07
18	40.0	0.0	6.80e-07
21	30.0	0.0	6.80e-07
23	30.0	30.0	6.40e-07
25	30.0	40.0	6.40e-07
26	33.3	33.3	6.40e-07
28	30.0	30.0	6.60e-07
32	30.0	30.0	6.60e-07
33	33.3	33.3	6.60e-07
37	30.0	30.0	6.60e-07
39	30.0	30.0	6.60e-07
40	0.0	30.0	6.60e-07
42	Harvest	0	
43		Harvest	

Plants were exposed to natural light. Seeds of arugula, lamb's lettuce, and spinach germinated in a horticultural substrate and were then moved in the soil pot after sprouting. Each plant was initially irrigated with fresh water and then exposed to the injection of contaminated water. Sets of five plants of each soil were also irrigated with solute-free water to test the possible impact of the compounds on plant growth. The measured CBZ inflow concentration varied between 6.4e-07 and 6.8e-07 g/cm^3 (Table 2). After exposure, plants were removed from the soil, rinsed, and divided into roots and shoots for the next chemical analysis, which was carried out using the liquid chromatography-tandem mass spectrometry. Before the sample

Table 3
Parameters and their bounds used in the experimental validation and global sensitivity analysis of the coupled HYDRUS-dynamic plant uptake model

Parameter[a]	Lamb's lettuce	Spinach	Arugula	Sensitivity analysis
θ_r (cm^3/cm^3)		0.08		(0.06, 0.10)
θ_s (cm^3/cm^3)		0.39		(0.30, 0.50)
α (cm^{-1})		0.05		(0.01, 0.1)
n (−)		1.22		(1.1, 2.0)
K_s (cm/day)		52		(20, 100)
ρ_b (g/cm^3)		1.09		(1, 1.3)
λ_L (cm)		2		(1, 4)
K_{fCBZ} ($cm^{3\beta}.\mu g^{1-\beta}.g^{-1}$)		2.97		(2, 5)
β_{CBZ} (−)		0.88		(0.7, 1.0)
μ_{LCBZ} (day^{-1})		0.0047		(0.001, 0.01)
μ_{SCBZ} (day^{-1})		0.0047		(0.001, 0.01)
P0 (cm)	−3	−3	−3	(−10, 0)
POpt (cm)	−20	−45	−45	(−35, −11)
P2H (cm)	−200	−200	−200	(−300, −100)
P2L (cm)	−800	−800	−800	-
P3 (cm)	−8000	−8000	−8000	-
Roots				
W (cm^3/g_{fw})	0.89	0.85	0.85	(0.8, 0.9)
L (g_l/g_{fw})	0.015	0.01	0.01	(0.005, 0.025)
M^{max} (g_{fw})	126	206	149	(100, 300)
M^0 (g_{fw})	4	10	4	(1, 20)
K^{gr} (day^{-1})	0.15	0.165	0.15	(0.08, 0.26)
τ_{11} (day^{-1})	0.15	0.165	0.026	(0.05, 0.3)
τ_{21}' (day^{-1})	0.11	0.133	0.023	-
τ_{31}' (day^{-1})	0.026	0.026	0.0026	-
τ_{22} (day^{-1})	0.004	0.004	0.004	-
Shoots				
W (cm^3/g_{fw})	0.89	0.85	0.86	(0.8, 0.9)
L (g_l/g_{fw})	0.015	0.01	0.01	(0.005, 0.025)
M^{max} (g_{fw})	440	819	723	(500, 1,000)
M^0 (g_{fw})	18	50	60	(10, 100)
K^{gr} (day^{-1})	0.15	0.165	0.15	(0.08, 0.26)
τ_{11} (day^{-1})	0.45	0.355	0.026	(0.05, 0.3)
τ_{21}' (day^{-1})	0.37	0.315	0.023	–
τ_{31}' (day^{-1})	0.07	0.035	0.0026	–
τ_{22} (day^{-1})	0.004	0.004	0.004	–
$A_{harvest}$ (cm^2)	47.5	65.6	48.9	–
$LAI_{harvest}$ (−)	1.9	2.6	2.0	–
Compounds				
$\log K_{OW}$ (CBZ) (−)		2.25		(2.0, 2.8)
$\log K_{OW}$ (EPX) (−)		1.26		-
$\log K_{OW}$ (OXC) (−)		1.11		-
$m_{(CBZ)}$ (g/mol)		236.27		-
$m_{(EPX)}$ (g/mol)		252.28		-
$m_{(EPX)}$ (g/mol)		252.28		-

[a] θ_s and θ_r are the saturated and residual water contents, respectively, α and n are the empirical van Genuchten-Mualem shape parameters, K_s is the saturated hydraulic conductivity, and P0, POpt, P2H, P2L, and P3 are Feddes' parameters.
CBZ = carbamazepine, EPX = 10,11-epoxide, LAI = Leaf Area Index.

extraction, the fresh and dry weights of roots and shoots, as well as the one-sided leaves area, were determined.

2.5.2. Model Setup

The one-dimensional model HYDRUS-1D is used to simulate transport processes in the soil. The 5.5-cm deep soil profile is discretized in 100 finite elements. An atmospheric boundary condition is applied at the soil surface using (a) irrigation and potential evapotranspiration fluxes, (b) a prescribed zero pressure head (i.e., full saturation) during ponding, and (c) equilibrium between the soil surface pressure head and the atmospheric water vapor pressure when the atmospheric evaporative demand cannot be met. A seepage face boundary condition is set at the bottom of the pot. This condition assumes that the boundary flux remains zero as long as the pressure head is below a certain threshold value, h_{seep}. However, when the lower end of the soil profile reaches this value, h_{seep} is imposed at the lower boundary and outflow is calculated accordingly. In the present study, h_{seep} is set to 1 cm to simulate the accumulation of water in the plate under the pot. The concentration flux across the top boundary is simulated using the classic Cauchy-type boundary condition, while a zero concentration gradient is imposed at the bottom. The initial pressure head is assumed to be constant and equal to −100 cm in the entire model domain. The soil is considered solute free at the beginning of the simulation.

Parameters used in the experimental validation are listed in Table 3. The unimodal van Genuchten-Mualem model (van Genuchten, 1980) is used to describe the soil hydraulic properties, which are obtained from the measured particle size distribution and soil bulk density ρ_b (grams per centimeter) using pedotransfer functions from ROSETTA (Schaap et al., 2001). The piecewise linear Feddes function describes the root water stress (Feddes et al., 1978) and regulates actual transpiration. Feddes' parameters (i.e., P0, POpt, P2H, P2L, and P3 in Table 3) are taken from the literature (Wesseling et al., 1991) and slightly adjusted to better reproduce measured data. Reference evapotranspiration is partitioned into potential evaporation and transpiration using the LAI. Growth rates are in line with values reported by Glenn et al. (1984) and Gent (2002). Final measured roots and shoots wet and dry masses, as well as one-sided leaves area—which averaged to an area of 1 m^2—are used to constrain equation (6).

The advection-dispersion-reaction equation (equation (26)) is used to simulate the transport of CBZ in the soil. The effect of molecular diffusion is neglected. The solute dispersivity λ_L is set to 2 cm. In their study, Kodešová et al. (2015) reported nonlinear equilibrium adsorption of CBZ on Haplic Chernozem, which can be described using the Freundlich adsorption isotherm

$$s_i = K_f C_i^{\beta}, \tag{28}$$

where K_f and β are empirical coefficients. Measured data show that the EPX is the only CBZ metabolite detected in the soil during the experiment. Thus, the CBZ degradation process in the soil is simulated using a sequential decay chain with first-order rate coefficients, μ_{LCBZ} and μ_{SCBZ} (T^{-1}), that account for the transformation of CBZ in EPX in the liquid and solid phases, respectively. Degradation of CBZ in this soil was studied by Kodešová et al. (2016). In this study, the degradation half-life was larger than 1,000 d, that is, μ_{LCBZ} and μ_{SCBZ} were lower than 0.0007 day^{-1}.

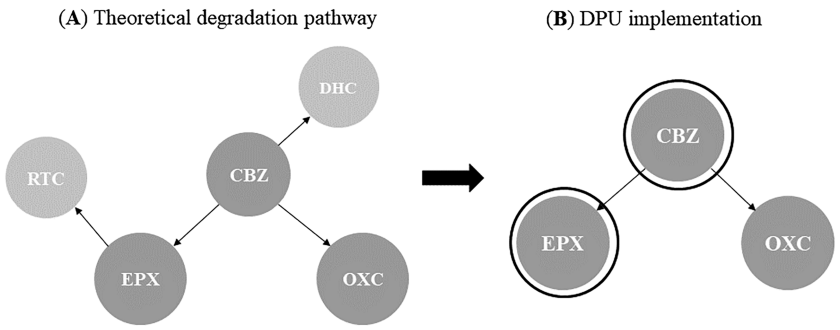

(C) Metabolization matrix for the jth compartment

$$\mathbf{\Omega}_j = \begin{Bmatrix} -\tau_{11} C_{CBZ,j} + 0.0 + 0.0 \\ +\tau_{21}{}' C_{CBZ,j} - \tau_{22} C_{EPX,j} + 0.0 \\ +\tau_{31}{}' C_{CBZ,j} + 0.0 - 0.0 \end{Bmatrix}$$

Figure 3. A schematic of the (a) theoretical degradation pathway of carbamazepine in plants, (b) the dynamic plant uptake implementation, (c) and the metabolization matrix for the jth compartment. The black circle indicates the compound degradation in by-products, which are not of interest in the analysis (i.e., reaction yield).

However, final concentrations of EPX in soils in the case of the pot greenhouse experiment (Kodešová et al., 2016) indicated higher degradation rates. Therefore a new degradation experiment was carried out with fresh soil, which was preincubated with water (20 °C) before application of pharmaceuticals. Resulting half-life was 0.0047 day^{-1}. The same sorption parameters are assumed for EPX, whose further degradation in the soil is neglected (Koba et al., 2016).

Plants are conceptualized in two compartments: roots and shoots. No CBZ was present in the greenhouse during the experiment and thus gaseous uptake and particle deposition are neglected. Similarly, volatilization is excluded from modeling due to the nonvolatile behavior of CBZ. Octanol-water partition coefficients are obtained using the U.S. Environmental Protection Agency Estimation Programs Interface suite program (U.S. EPA, 2013). Water contents of plants' compartments are estimated from the measured fresh and dry weights of roots and shoots and slightly adjusted so that modeled and measured concentrations better match. The lipid contents are set based on literature values reported for leafy vegetables (Legind et al., 2011; Legind et al., 2012; Trapp & Eggen, 2013; Wen et al., 2016) and slightly increased to compensate the underestimation of the sorption introduced by equation (8). Contrary to the soil, multiple CBZ metabolites were observed in plants. In particular, EPX and OXC were the most significant by-products while only small concentrations of trans-10,11-dihydro-10,11-dihydroxy carbamazepine (RTC) and 10,11-dihydro carbamazepine (DHC) were observed. In the present study, we focus only on the transformation of CBZ in its main active metabolites, EPX and OXC. RTC and DHC are not of immediate interest in the analysis; and thus, they are not explicitly included in the DPU metabolization chain but instead considered in the reaction yield of EPX and CBZ. Theoretical degradation pathways of CBZ in plants and its conceptual implementation in the DPU model are shown in Figure 3. Input concentrations, as well as sorption parameters, are converted to molar units before executing the model, while output concentrations are reported in nanogramg per gram for visualization purposes.

2.5.3. Global Sensitivity Analysis

Accurate integrated models can be used to understand how different components of the simulated process interact and to identify the key driving factors. A classic example is to perform a sensitivity analysis on the model to investigate the impact of different parameters on some variables of interest. The sensitivity analysis is frequently used in modeling studies under different settings and aims (e.g., Brunetti et al., 2016; Brunetti et al., 2017; Brunetti, Šimůnek, & Bautista, 2018; Brunetti, Šimůnek, Turco, & Piro, 2018). In the present study, we apply a global sensitivity analysis to identify the most important factors among soil, plant, and chemical parameters that drive the accumulation of CBZ in spinach shoots. To this aim, the developed soil-plant model is coupled with a modified version of the Morris method (Morris, 1991) proposed by Campolongo et al. (2007).

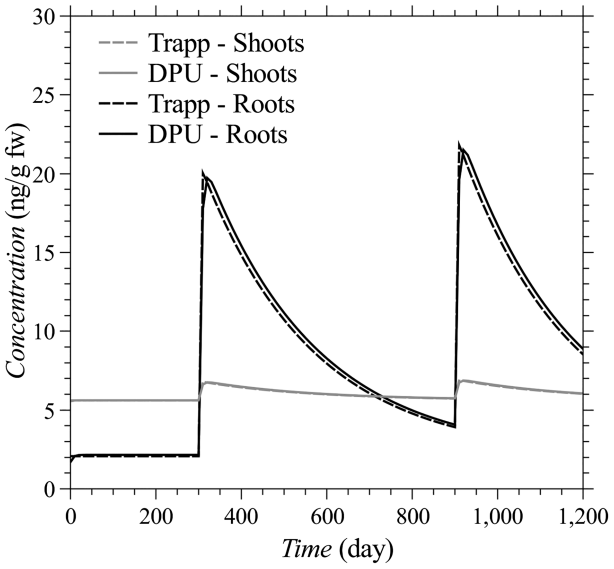

Figure 4. A comparison between the simulated solute concentrations in roots (black) and shoots (gray) of the Trapp (dashed lines) and dynamic plant uptake (DPU; solid lines) models, respectively.

The Morris method (Morris, 1991) belongs to the class of *screening methods*. *Screening methods* aim to provide qualitative sensitivity measures for different factors using a relatively small number of model evaluations. In general, the Morris method is a one-factor-at-a-time local method since it computes the *elementary effect* by changing only one factor at a time. However, it can be viewed as a global method since it averages several elementary effects computed at different points in the parameter space, providing a qualitative measure of the importance and interactions of different factors. The main outcomes of the analysis are two sensitivity indices, σ and μ^*, which summarize the interaction and overall importance of the parameter, respectively. High values of these sensitivity indices indicate a significant influence of the parameter on the variable of interest. To interpret the results by simultaneously taking into account both sensitivity measures, Morris suggested their graphical representation in the (μ^*–σ) plane.

The same model settings used in the experimental validation for spinach are used in the sensitivity analysis. Since the main aim is to identify factors driving the accumulation of CBZ in shoots, its metabolites are neglected, and the metabolization matrix is reduced to a single scalar value for each compartment. Furthermore, preliminary numerical simulations have shown that during the experiment, the soil was in nearly saturated conditions; thus, only the "anaerobiosis" and "optimal" pressure head values in the Feddes' model, P0 and POpt, are included in the sensitivity analysis, which reduces the number of screened parameters to 27. Table 3 reports these screen parameters with their ranges of variation. A sample size of 200 is used to generate the initial sample, leading to a total of 5,400 numerical simulations. The analysis is carried out using the Python programming language. For each sample, the code overwrites the input, executes the coupled HYDRUS-DPU model, and stores the value of the final CBZ concentration in shoots in a preassigned array. Finally, the sensitivity indices are calculated, and the μ^*–σ plot is used to target important factors.

3. Results

3.1. Theoretical Validation

Results of the theoretical validation are reported in Figure 4, which shows a comparison between the simulated solute concentrations in roots (black) and shoots (gray) for the Trapp (dashed lines) and DPU (solid lines) models, respectively. Simulated concentrations overlap, thus confirming the correctness of the DPU model implementation. The implemented model can accurately reproduce both the solute accumulation in roots after the pulse injection and the following decrease induced by the metabolization. The low compound translocation in shoots due to the relatively high solute lipophilicity (i.e., $\log K_{OW} = 2.00$) is also correctly described by the model. The implicit time discretization method used to solve the mass-balance equation (equation (4)) is responsible for the slight smoothing of results observed in the roots compartment (Figure 4) and explains the negligible deviation between the Trapp and DPU models. Nevertheless, it can be concluded that the DPU model implementation is theoretically correct, numerically stable, and can be used for further analyses.

3.2. Experimental Validation

The main outcomes of the experimental validation are reported in Figure 5, which shows a comparison between the simulated and measured concentrations of CBZ and its main metabolites in the soil, roots, and shoots of lamb's lettuce, spinach, and arugula. Overall, the coupled HYDRUS-DPU model satisfactorily reproduces the final accumulation of different compounds in the soil and plants' tissues. The highest deviation is observed in the lamb's lettuce scenario, for which the model underestimates the high enzymatic biodegradation observed in shoots (Kodešová et al., 2019b). Such effect, which is more pronounced for the EPX, can be mainly related to some bias in the assumed first-order metabolization coefficients, as well as to plausible uncertainties in soil and plant input parameters. Nevertheless, simulated compound concentrations are in the measurement uncertainty ranges, suggesting an overall good performance of the model. This is further

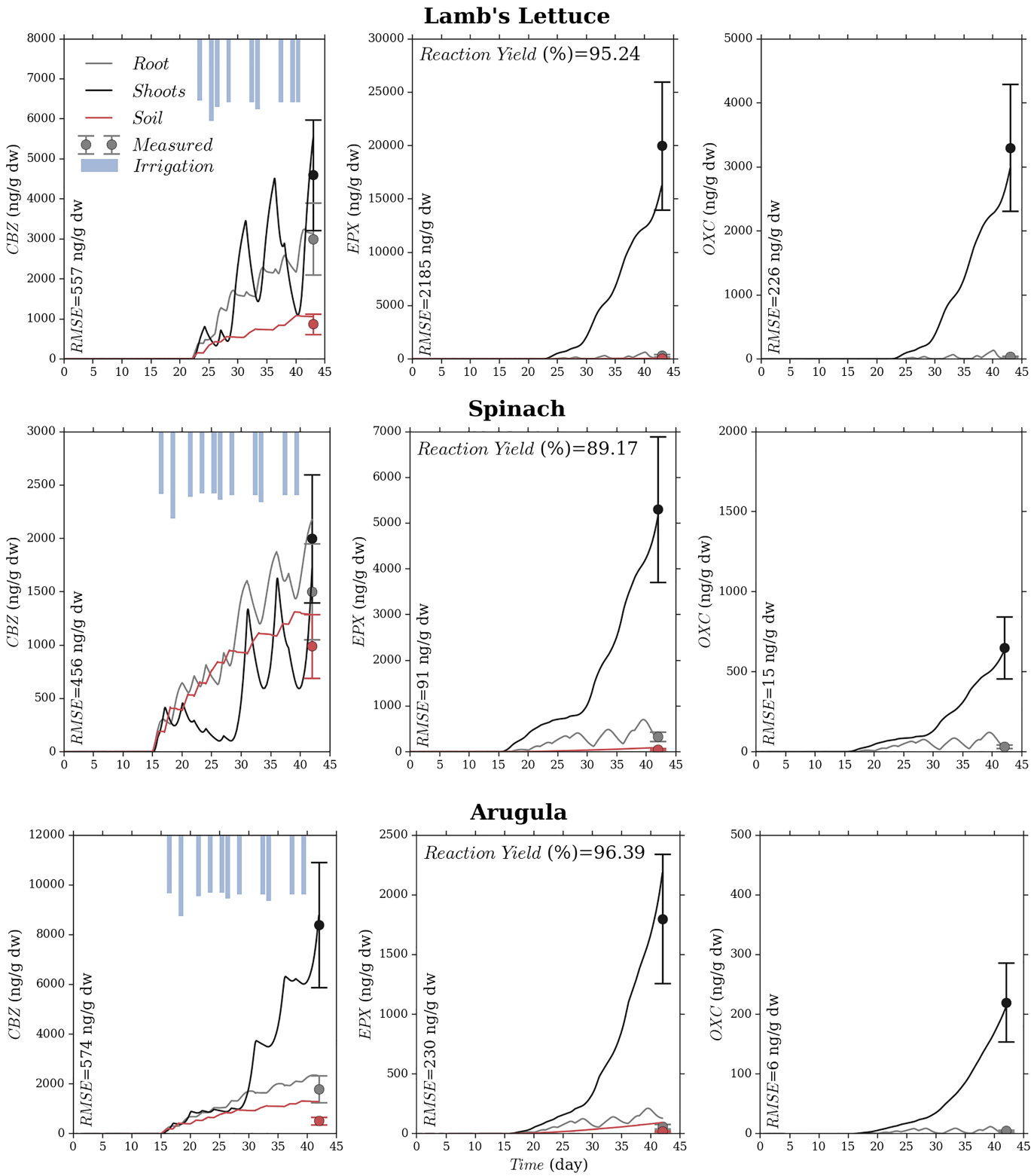

Figure 5. A comparison between the simulated (solid lines) and measured (dots) concentrations of carbamazepine (left) and its main metabolites 10,11-epoxide (middle) and oxcarbazepine (right) in the soil (red), roots (gray) and shoots (black) of lamb' lettuce (top), spinach (middle), and arugula (bottom). The blue bars are the solute irrigation fluxes (Table 2). The error bar indicates the estimated 30% uncertainty of the measurement method, according to Kodešová et al. (2019b). The reaction yield indicates the amount of metabolized carbamazepine converted in 10,11-epoxide and oxcarbazepine.

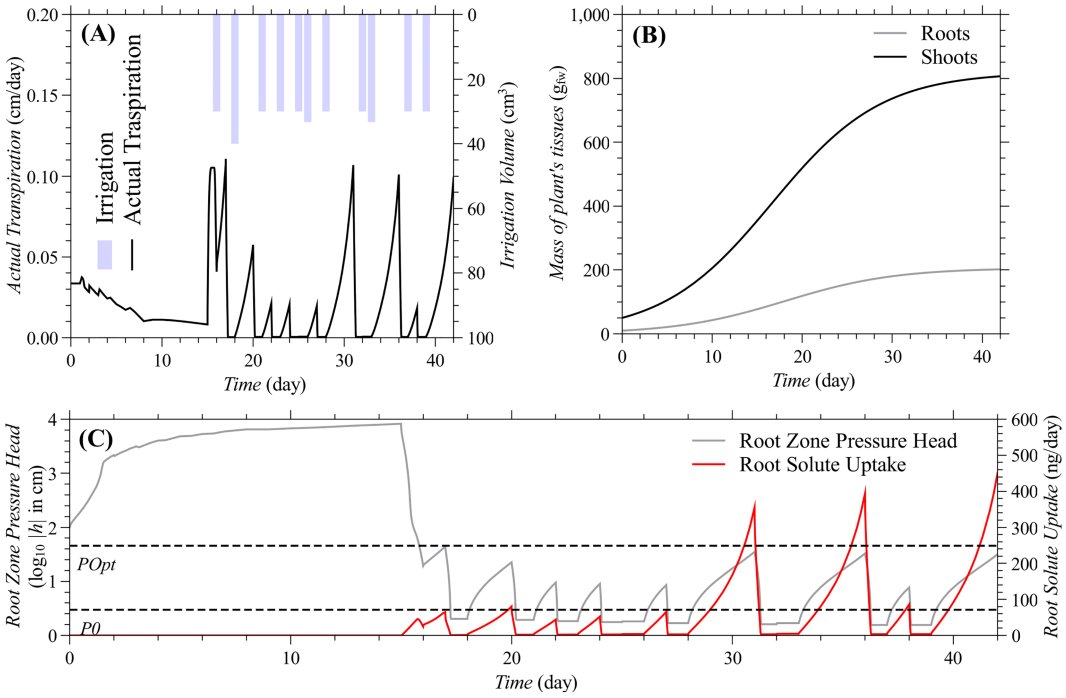

Figure 6. (a) Simulated actual transpiration (black line) and irrigation volumes (blue bars); (b) simulated roots (gray line) and shoots (black line) masses; (c) the average root zone pressure head (gray line) and root solute uptake (red line) in the spinach modeling scenario. P0 and POpt are the "anaerobiosis" and "optimal" pressure head values in the Feddes' model.

confirmed by the higher fitting accuracy achieved in the spinach and arugula modeling scenarios. Here, the model accurately reproduces both the biodegradation pathways of CBZ in roots and shoots while some overestimation is evident in the soil. Such behavior is more pronounced for arugula, for which the model overpredicts both the CBZ and EPX concentrations, thus suggesting that the bias mainly stems from potential inaccuracies in the description of soil transport processes. On the other hand, the compounds' bioaccumulation in spinach is well described in all model compartments, though the CBZ concentration in the soil is again slightly overestimated.

One of the main advantages of the proposed coupled model is its ability to provide a dynamic description of transport and degradation processes in the soil-plant continuum, which is crucial to developing a better understanding of physical processes happening during the experiment. When irrigation begins in the experiment, DPU starts and CBZ is translocated with transpiration streams to the shoots. At the same time, it is biodegraded by plant's enzymes in its by-products, which are compartmented in leaves and eventually further metabolized. The fluctuations in the simulated concentrations are mainly due to the actual transpiration patterns induced by the variably saturated conditions in the soil. This is clearly shown in Figure 6, which shows the simulated root zone pressure head and actual root solute uptake for the spinach modeling scenario. Model results suggest that irrigation caused nearly saturated conditions in the pot, which induced anaerobic stress (as defined by Feddes' stress response function) on plant's roots, thereby limiting water and solute uptake (Figure 6). This is particularly evident in spinach roots and shoots between Days 20 and 30 of the simulated period when the CBZ concentration declines (Figure 5) due to enzymatic biodegradation and simultaneous negligible supply of contaminant with transpiration water. After this period, the pressure head decreases below the anaerobiosis pressure head value and DPU starts again with a subsequent translocation and compartmentation of EPX and OXC in leaves.

Despite the promising results, it must be emphasized that the amount and information content of measured data available for validating the model was rather limited. For this reason, we avoid numerical parameter optimization, which could improve the quality of the fit but would likely lead to unphysical parameter values and high predictive uncertainty. In this perspective, future research will focus on proper Bayesian model validation against highly informative measurements from selected experiments, which are already

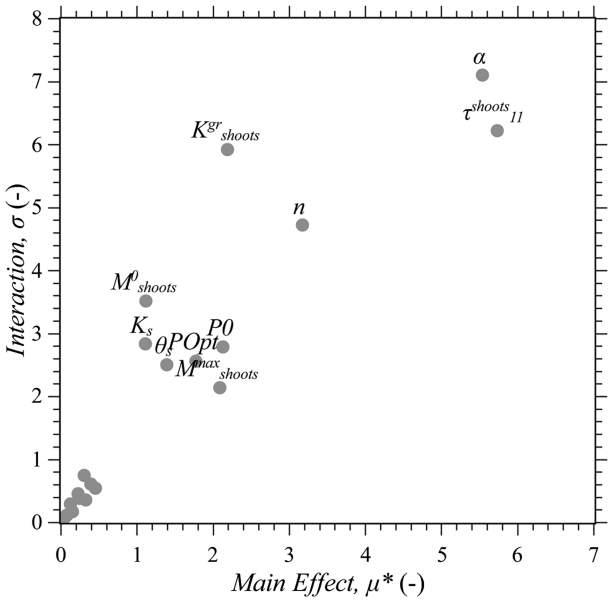

Figure 7. Scatter plots of the Morris sensitivity measures for various soil hydraulic, plant, and solute transport parameters.

ongoing at the Czech University of Life Sciences, Prague. Nevertheless, this preliminary experimental validation demonstrates that the developed model shows good promise for describing transport processes in the soil-plant continuum.

3.2.1. Global Sensitivity Analysis

The results of the experimental validation suggest an important role of the soil in the compounds' translocation process in plants. To further investigate this aspect, a global sensitivity analysis is performed to screen factors influencing the accumulation of CBZ in shoots. Results of the analysis, carried out using the Morris method, are summarized in the scatter plot $\mu^*-\sigma$ shown in Figure 7.

Three parameter groups can be identified from the distribution of sensitivity measures. The first group, in order of importance, includes the shoots growth rate K^{gr}_{shoots}, the van Genuchten-Mualem shape parameters, α and n, and the first-order degradation rate in the shoots, τ^{shoots}_{11}. The effect of the latter is expected since it directly regulates simulated biodegradation of CBZ in the shoots, thus modulating the sink term in equation (4). The outcome for α and n holds more interest, further confirming findings of the experimental validation on the role of soil hydraulic behavior on solute translocation in plants during the experiment. Parameters α and n describe the start and magnitude of the desaturation process in the soil-water retention curve, thus governing the simulated soil retention capacity. In particular, under nearly saturated conditions, small perturbations of α, generated by the Morris sampling process, propagate in the simulated root zone pressure head, which now oscillates near the anaerobiosis point defined in the Feddes' model, thus strongly influencing actual root water and solute uptake. Such behavior is exacerbated in combination with simultaneous changes of n, as demonstrated by the high interaction effect, σ, calculated for these parameters. This suggests that an accurate estimation of these parameters would significantly increase the model predictive capabilities and reduce the overall uncertainty. Similarly, the shoots growth rate, K^{gr}_{shoots}, exhibits a high interaction potential, as it is mainly involved in the compound's dilution effect in the plant. In this case, few measurements of the plant mass during its growth stage would be sufficient to characterize the plant's growth and thus to better constrain the model.

The second group includes the initial and final shoots masses, M^{0}_{shoots} and M^{max}_{shoots}, the saturated water content and hydraulic conductivity, θ_s and K_s, respectively, and the anaerobiosis and optimal pressure head values in the Feddes' model, P0 and POpt, respectively. As expected, the Feddes' parameters have a significant impact on CBZ bioaccumulation in the shoots since they regulate simulated actual root water uptake, and thus transpiration streams, in nearly saturated conditions. In such circumstances, θ_s and K_s strongly influence the soil hydraulic behavior, which in turn affects the root uptake process. Finally, the dilution effect mainly explains the moderate sensitivity of the simulated CBZ accumulation to M^{0}_{shoots} and M^{max}_{shoots}.

The third group includes all remaining parameters, which for physical reasons have proven to have a limited effect on the variable of interest. For instance, the residual water content θ_r has a negligible impact on the soil hydraulic behavior in wet conditions, which were observed during the experiment. Similarly, in the analyzed modeling scenario, the octanol-water partition coefficient log K_{OW} has a limited influence since its range of variation does not significantly modify lipophilicity of the compound. While it is likely that wider bounds could lead to a different sensitivity ranking, its scientific meaning could be highly questionable due to the adoption of an unphysical value of log K_{OW} for CBZ, whose value is known and reported in the literature. Interestingly, solute transport and adsorption parameters exhibit low sensitivity measures. Such behavior can be partially explained by the limited volume of the pot, as well as by the overall experimental conditions.

It should be emphasized that the present sensitivity analysis is aimed at providing insight into the most important factors affecting DPU of CBZ during a specific experiment. Results should thus not be regarded

as general but should instead be restricted to a particular investigated modeling scenario. Different model settings can certainly lead to different results. However, the present analysis demonstrates how the developed soil-plant model can be used in conjunction with advanced statistical techniques to better understand physical processes.

4. Discussion

4.1. Integrated Soil-Plant Model

The analysis demonstrates how the implementation of the DPU module in the HYDRUS model significantly extends its capabilities by providing an integrated modeling environment for contaminant risk assessment in the soil-plant continuum. The adopted coupling strategy is numerically stable, computationally effective, and mathematically accurate, as demonstrated by the theoretical and experimental validation. Furthermore, the comprehensive description of the contaminant transport in the soil and plant can be used in conjunction with advanced statistical tools, such as global sensitivity and Bayesian analyses, to gain insights into the investigated process and to better explain interactions between the soil and plant domains. Additionally, the modeling approach—based on multiple metabolization matrices—increases modeling flexibility. To continue these advances, further layers of complexity can be added to the model by refining the description of enzymatic and bacterial biodegradation in the plant's tissues using the Michaelis-Menten and Monod kinetics, respectively. The former has been observed for the enzymatic degradation of cyanide in plants (Larsen et al., 2004; Yu et al., 2004) and the exclusion of salt NaCl and NaF from roots (Clausen et al., 2015; Trapp et al., 2008). Future developments could also include an option to use an optimal plant growth function (equation (6)) and reduce the growth due to various stresses such as saturation, osmotic, or chemical stresses. A comparison with more simplistic numerical approaches (e.g., tipping bucket models) is recommended to assess, under what conditions, this increase in the soil-plant model complexity is justifiable.

One of the main limitations of the proposed model is the simplification of the plant physiology compared to other soil-plant models (e.g., Fatichi et al., 2019, 2016; Huang et al., 2018, 2017; Huber et al., 2014; Manoli et al., 2017; Werner & Dubbert, 2016), some of which provide a detailed multidimensional mechanistic description of the xylem and phloem flow, photosynthesis, carbon allocation, leaf-level gas exchange, energy balance, etc. However, this increase in the model complexity requires highly informative measurements and poses computational cost issues, especially for model calibration, that can undermine its usability for practical applications at the plot scale. Such problems are mitigated in the model developed in this study, which can be used in various applications, such as phytoremediation involving uptake and metabolization processes of toxic compounds from contaminated soils (e.g., Ouyang, 2002), pesticides fate assessment (e.g., Legind et al., 2011), remediation of contaminated groundwater plumes (e.g., Hong et al., 2001), assessment of salinity in agricultural arid areas (e.g., Trapp et al., 2008), and air pollution removal by urban vegetation (e.g, Yang et al., 2008). To further extend the range of the model applicability, future research should focus on the modification of the model structure to consider DPU of electrolytes and refine the description of the root uptake mechanism of large molecules (Kumar & Gupta, 2016).

Nevertheless, this study cannot cover all potential modeling scenarios, and thus, additional research is needed to assess the robustness of the proposed approach under various operating conditions. In particular, the role of numerical stiffness on the choice of the time step must be clarified, which in turn affects the stability of the overall scheme. In the proposed coupling strategy, the HYDRUS internal solver dictates the time step for the DPU module. The time step is selected in HYDRUS based on convergence criteria of the numerical solution of the Richards equation and stability criteria of the numerical solution of the convection-dispersion equation. Thus, the choice of the time step during the simulation mainly depends on the dynamics of soil transport processes, which are assumed to be happening at a finer time scale compared to the plant translocation. Such an assumption is expected to hold in the majority of modeling scenarios. However, potential numerical issues could arise when simulating DPU of highly volatile compounds from soils in nearly steady-state conditions. Under such circumstances, the time step chosen by HYDRUS could not be sufficiently small so as to catch the dynamics of the volatilization process in the plant. Thus, we recommend future studies to focus on this aspect to target eventual instability problems, as well as on a better description of nonequilibrium sorption and biodegradation in plants.

4.2. The Key Role of Soil Transport Processes

The results of the experimental validation and global sensitivity analysis emphasize the role of soil transport processes on the compound's bioaccumulation in plants. Such an effect is mainly explained by the influence of unsaturated conditions on actual transpiration streams, which govern the contaminants' translocation in plants. Existing DPU models greatly simplify the unsaturated hydraulic behavior of the root zone using questionable coarse theoretical conceptualizations. A classic example is a use of tipping bucket models (Legind et al., 2012; Trapp & Eggen, 2013), which suffer from multiple theoretical and practical limitations (Emerman, 1995; Scanlon, Christman, et al., 2003). Our implementation, based on the HYDRUS model, overcomes such limitations, providing a modeler the possibility to mechanistically simulate single porosity and preferential flows, as well as equilibrium and nonequilibrium solute transport processes. The results of this study demonstrate that such modeling features are crucial to understanding how the interaction between variably saturated flow conditions and the plant's respiration affect dynamic root water and solute uptake (Figure 6).

4.3. Model Complexity and Uncertainty Assessment

The high modeling flexibility of the developed soil-plant model leads to high model parameterization. Several parameters are needed to describe physical and chemical processes in the soil and plant. Furthermore, the use of multiple metabolization matrices for the simulation of differentiated biodegradation in plant's tissues introduces additional layers of model complexity, which are certainly a valuable tool for the modeler when the main aim of the analysis is the model-based design (e.g., Lange et al., 2015). Under such circumstances, parameters are established from the literature, and the model is used to design the system and simulate its future behavior under actual conditions.

The situation is radically different when the main goal of the analysis is predictive modeling. Under such circumstances, parameters must be inferred from measured data through model calibration. However, highly parameterized models often suffer from poor predictive capabilities due to high parameter uncertainty, mainly stemming from the limited information content of measured data. The situation can be further worsened when simulating highly nonlinear processes, as in the DPU model. For these reasons, the information content of measured data is critical to strengthening the generalizability of the coupled soil-plant model, which must be assessed through a Bayesian calibration framework. In the present study, we decided to avoid a perfunctory model calibration due to the limited amount of available measured data, which would lead to poor model generalizability. Therefore, we recommend future research to focus on a more rigorous uncertainty assessment using more comprehensive measured data sets to clarify how the high parameterization of the soil-plant model affects its predictive capabilities in real case studies. A soil-plant column experiment under variable atmospheric conditions (e.g., a climate chamber) and different solute injections that would include measurements of pressure heads and soil water contents at multiple depths, as well as solute concentrations in plants, would be of great interest. The information content of the experimental data set could be increased by targeted laboratory measurements, such as unsaturated hydraulic properties (e.g., Peters & Durner, 2008) and solute sorption on plant's tissues (e.g., Li et al., 2005), which could then be used as prior information for subsequent inverse parameter estimation using transient data. We advocate that such an approach should be ubiquitous when using numerical simulations of DPU of selected compounds. Thus far, research in this field has focused on the use of conceptual models in combination with local sensitivity analyses, which—despite good intentions—suffered from theoretical (Emerman, 1995; Scanlon, Christman, et al., 2003) and statistical limitations (Saltelli & Annoni, 2010) to capture the main physical aspects of the investigated process.

5. Conclusions

The main aim of the present study was to develop a comprehensive model capable of providing a mechanistic description of transport and reaction processes in the soil-plant continuum. The results of the multilevel numerical analysis demonstrate that the developed model shows good promise for reproducing physicochemical processes involved in DPU of chemicals from contaminated soils. The possibility of having an integrated mechanistic description of both soil and plant behaviors fills a significant scientific gap in this field, often characterized by fragmented research experiences. For example, the developed model can be used in environmental applications to simulate uptake of chemicals from contaminated sites and their

translocation and transformation in the soil-plant continuum in a comprehensive contaminant risk assessment. We certainly do not expect this study to be exhaustive in terms of exploring all plausible modeling scenarios nor conclusive in the highly dynamic scientific field of soil-plant modeling. The numerical description of plant physiology can certainly be improved, and the model stability, usability, and generalizability should be further explored. The latter is of especially great importance since the high parameterization of the developed model can result in poor predictive capabilities. As we pointed out in the section 4, further model testing and experimental validation are needed to assess this and other aspects. Nevertheless, the high modeling flexibility of the proposed numerical approach is undoubtedly a very useful tool for developing reliable mitigation strategies for environmental pollution problems.

Acknowledgments
Authors acknowledge the financial support of the Czech Science Foundation Project 17-08937S, behavior of pharmaceuticals in the soil-water-plant system. The work was also supported from European Structural and Investment Funds, Operational Programme Research, Development and Education and Ministry of Education, Youth and Sports projects supporting the development of international mobility of research staff at CULS Prague (CZ.02.2.69/0.0/0.0/16_027/0008366), and NutRisk (CZ.02.1.01/0.0/0.0/16_019/0000845). The data that support the findings of this study are available at https://zenodo.org/record/3275850#.XSSrHY_ONPY.

References

Barac, T., Taghavi, S., Borremans, B., Provoost, A., Oeyen, L., Colpaert, J. V., et al. (2004). Engineered endophytic bacteria improve phytoremediation of water-soluble, volatile, organic pollutants. *Nature Biotechnology*. https://doi.org/10.1038/nbt960

Bertrand, J., Laffont, C. M., Mentré, F., Chenel, M., & Comets, E. (2011). Development of a complex parent-metabolite joint population pharmacokinetic model. *AAPS Journal*. https://doi.org/10.1208/s12248-011-9282-9

Boote, K. J., Sau, F., Hoogenboom, G., & Jones, J. W. (2008). Experience with Water Balance, Evapotranspiration, and Predictions of Water Stress Effects in the CROPGRO Model. In L. R. Ahuja, V. R. Reddy, S. A. Saseendran, & Q. Yu (Eds.), *Response of Crops to Limited Water: Understanding and Modeling Water Stress Effects on Plant Growth Processes, Adv. Agric. Syst. Model. 1* (pp. 59–103). Madison, WI: ASA, CSSA, SSSA. https://doi.org/10.2134/advagricsystmodel1.c3

Briggs, G. G., Bromilow, R. H., & Evans, A. A. (1982). Relationships between lipophilicity and root uptake and translocation of non-ionised chemicals by barley. *Pesticide Science*, *13*(5), 495–504. https://doi.org/10.1002/ps.2780130506

Brodersen, C. R., Roddy, A. B., Wason, J. W., & McElrone, A. J. (2019). Functional status of xylem through time. *Annual Review of Plant Biology*, *70*(1), 407–433. https://doi.org/10.1146/annurev-arplant-050718-100455

Broyden, C. G. (1969). A new method of solving nonlinear simultaneous equations. *Computer Journal*, *12*(1), 94–99. https://doi.org/10.1093/comjnl/12.1.94

Brunetti, G., Porti, M., & Piro, P. (2018). Multi-level numerical and statistical analysis of the hygrothermal behavior of a non-vegetated green roof in a mediterranean climate. *Applied Energy*, *221*, 204–219. https://doi.org/10.1016/J.APENERGY.2018.03.190

Brunetti, G., Saito, H., Saito, T., & Šimůnek, J. (2017). A computationally efficient pseudo-3D model for the numerical analysis of borehole heat exchangers. *Applied Energy*, *208*, 1113–1127. https://doi.org/10.1016/j.apenergy.2017.09.042

Brunetti, G., Šimůnek, J., & Bautista, E. (2018). A hybrid finite volume-finite element model for the numerical analysis of furrow irrigation and fertigation. *Computers and Electronics in Agriculture*, *150*, 312–327. https://doi.org/10.1016/J.COMPAG.2018.05.013

Brunetti, G., Šimůnek, J., Bogena, H., Baatz, R., Huisman, J. A., Dahlke, H., & Vereecken, H. (2019). On the information content of cosmic-ray neutron data in the inverse estimation of soil hydraulic properties. *Vadose Zone Journal*, *18*(1), 0. https://doi.org/10.2136/vzj2018.06.0123

Brunetti, G., Šimůnek, J., & Piro, P. (2016). A comprehensive numerical analysis of the hydraulic behavior of a permeable pavement. *Journal of Hydrology*, *540*, 1146–1161. https://doi.org/10.1016/j.jhydrol.2016.07.030

Brunetti, G., Šimůnek, J., Turco, M., & Piro, P. (2018). On the use of global sensitivity analysis for the numerical analysis of permeable pavements. *Urban Water Journal*, *15*(3), 269–275. https://doi.org/10.1080/1573062X.2018.1439975

Butcher, J.C., 2016. Numerical methods for ordinary differential equations, numerical methods for ordinary differential equations. https://doi.org/10.1002/9781119121534

Campolongo, F., Cariboni, J., & Saltelli, A. (2007). An effective screening design for sensitivity analysis of large models. *Environmental Modelling & Software*, *22*(10), 1509–1518. https://doi.org/10.1016/j.envsoft.2006.10.004

Cheyns, K., Mertens, J., Diels, J., Smolders, E., & Springael, D. (2010). Monod kinetics rather than a first-order degradation model explains atrazine fate in soil mini-columns: Implications for pesticide fate modelling. *Environmental Pollution*, *158*(5), 1405–1411. https://doi.org/10.1016/j.envpol.2009.12.041

Clausen, L. P. W., Karlson, U. G., & Trapp, S. (2015). Phytotoxicity of sodium fluoride and uptake of fluoride in willow trees. *International Journal of Phytoremediation*, *17*(4), 369–376. https://doi.org/10.1080/15226514.2014.910166

de Jong van Lier, Q., van Mentré, J. C., Durigon, A., dos Santos, M. A., & Metselaar, K. (2013). Modeling water potentials and flows in the soil-plantsystem comparing hydraulic resistances and transpiration reduction functions. *Vadose Zone Journal*, *12*(3). https://doi.org/10.2136/vzj2013.02.0039

Dumont, C., Mentré, F., Gaynor, C., Brendel, K., Gesson, C., & Chenel, M. (2013). Optimal sampling times for a drug and its metabolite using simcyp® simulations as prior information. *Clinical Pharmacokinetics*, *52*(1), 43–57. https://doi.org/10.1007/s40262-012-0022-9

Emerman, S. H. (1995). The tipping bucket equations as a model for macropore flow. *Journal of Hydrology*, *171*(1-2), 23–47. https://doi.org/10.1016/0022-1694(95)02735-8

U.S. EPA (2013). *Estimation Program Interface (EPI) Suite, v4.1. United States Environ*. Washington, DC, USA: Prot. Agency.

Eugenio, N. R., McLaughlin, M., & Pennock, D. (2018). *Soil pollution: A hidden reality*. Rome: FAO.

Fantke, P., & Juraske, R. (2013). Variability of pesticide dissipation half-lives in plants. *Environmental Science & Technology*, *47*(8), 3548–3562. https://doi.org/10.1021/es303525x

FAO, 2019. The future of food safety-First FAO/WHO/AU international food safety conference. Addis.

Fatichi, S., Manzoni, S., Or, D., & Paschalis, A. (2019). A Mechanistic model of microbially mediated soil biogeochemical processes: A reality check. *Global Biogeochemical Cycles*, *33*(6), 620–648. https://doi.org/10.1029/2018GB006077

Fatichi, S., Pappas, C., & Ivanov, V. Y. (2016). Modeling plant-water interactions: An ecohydrological overview from the cell to the global scale. *Wiley Interdisciplinary Reviews Water*, *3*(3), 327–368. https://doi.org/10.1002/wat2.1125

Feddes, R. A., Kowalik, P. J., & Zaradny, H. (1978). *Simulation of field water use and crop yield.*. Wageningen: PUDOC (Centre for agricultural publishing and documentation).

Gent, M. P. N. (2002). Growth and composition of salad greens as affected by organic compared to nitrate fertilizer and by environment in high tunnels. *Journal of Plant Nutrition*, *25*(5), 981–998. https://doi.org/10.1081/PLN-120003933

Glenn, E. P., Cardran, P., & Thompson, T. L. (1984). Seasonal effects of shading on growth of greenhouse lettuce and spinach. *Scientia Horticulturae (Amsterdam).*, *24*(3-4), 231–239. https://doi.org/10.1016/0304-4238(84)90106-7

Glick, B. R. (2010). Using soil bacteria to facilitate phytoremediation. *Biotechnology Advances*, *28*(3), 367–374. https://doi.org/10.1016/j.biotechadv.2010.02.001

Goldstein, M., Malchi, T., Shenker, M., & Chefetz, B. (2018). Pharmacokinetics in plants: Carbamazepine and its interactions with lamotrigine. *Environmental Science & Technology*, *52*(12), 6957–6964. https://doi.org/10.1021/acs.est.8b01682

Hanson, B. R., Šimůnek, J., & Hopmans, J. W. (2006). Evaluation of urea–ammonium–nitrate fertigation with drip irrigation using numerical modeling. *Agricultural Water Management*, *86*(1-2), 102–113. https://doi.org/10.1016/J.AGWAT.2006.06.013

Hartzell, S., Bartlett, M. S., & Porporato, A. (2017). The role of plant water storage and hydraulic strategies in relation to soil moisture availability. *Plant and Soil*, *419*(1-2), 503–521. https://doi.org/10.1007/s11104-017-3341-7

Herbst, M., Fialkiewicz, W., Chen, T., Pütz, T., Thiéry, D., Mouvet, C., et al. (2005). Intercomparison of flow and transport models applied to vertical drainage in cropped lysimeters. *Vadose Zone Journal*, *4*(2). https://doi.org/10.2136/vzj2004.0070

Hoffman, G. J., van Genuchten, M. T., & Metselaar, K. (1983). Soil properties and efficient water use: Water management for salinity control.. In H. M. Taylor, W. R. Jordan, & T. R. Sinclair (Eds.) *Limitations to Efficient Water Use in Crop Production*. American Society of Agronomy: Madison, WI(pp. 73–85). https://doi.org/10.2134/1983.limitationstoefficientwateruse.c5

Hong, M. S., Farmayan, W. F., Dortch, I. J., Chiang, C. Y., McMillan, S. K., & Schnoor, J. L. (2001). Phytoremediation of MTBE from a groundwater plume. *Environmental Science & Technology*, *35*(6), 1231–1239. https://doi.org/10.1021/es001911b

Huang, C. W., Domec, J. C., Palmroth, S., Pockman, W. T., Litvak, M. E., & Katul, G. G. (2018). Transport in a coordinated soil-root-xylem-phloem leaf system. *Advances in Water Resources*, *119*, 1–16. https://doi.org/10.1016/j.advwatres.2018.06.002

Huang, C. W., Domec, J. C., Ward, E. J., Duman, T., Manoli, G., Parolari, A. J., & Katul, G. G. (2017). The effect of plant water storage on water fluxes within the coupled soil–plant system. *New Phytologist*, *213*(3), 1093–1106. https://doi.org/10.1111/nph.14273

Huber, K., Vanderborght, J., Javaux, M., Schröder, N., Dodd, I. C., & Vereecken, H. (2014). Modelling the impact of heterogeneous rootzone water distribution on the regulation of transpiration by hormone transport and/or hydraulic pressures. *Plan and Soil*. *384*(1-2), 93–112. https://doi.org/10.1007/s11104-014-2188-4

Hung, H., & Mackay, D. (1997). A novel and simple model of the uptake of organic chemicals by vegetation from air and soil. *Chemosphere*, *35*(5), 959–977. https://doi.org/10.1016/S0045-6535(97)00182-3

Hurtado, C., Trapp, S., & Bayona, J. M. (2016). Inverse modeling of the biodegradation of emerging organic contaminants in the soil-plant system. *Chemosphere*, *156*, 236–244. https://doi.org/10.1016/j.chemosphere.2016.04.134

Jarvis, N., & Larsbo, M. (2012). MACRO (v5.2): Model use, calibration, and validation. *Transactions of the ASABE*, *55*(4), 1413–1423. https://doi.org/10.13031/2013.42251

Javaux, M., Couvreur, V., Vanderborght, J., & Vereecken, H. (2013). Root water uptake: From three-dimensional biophysical processes to macroscopic modeling approaches. *Vadose Zone Journal*, *12*(4). https://doi.org/10.2136/vzj2013.02.0042

Jellali, S., Diamantopoulos, E., Haddad, K., Anane, M., Durner, W., & Mlayah, A. (2016). Lead removal from aqueous solutions by raw sawdust and magnesium pretreated biochar: Experimental investigations and numerical modelling. *Journal of Environmental Economics and Management*, *180*, 439–449. https://doi.org/10.1016/j.jenvman.2016.05.055

Koba, O., Golovko, O., Kodešová, R., Klement, A., & Grabic, R. (2016). Transformation of atenolol, metoprolol, and carbamazepine in soils: The identification, quantification, and stability of the transformation products and further implications for the environment. *Environmental Pollution*, *218*, 574–585. https://doi.org/10.1016/j.envpol.2016.07.041

Kodešová, R., Grabic, R., Kočárek, M., Klement, A., Golovko, O., Fér, M., et al. (2015). Pharmaceuticals' sorptions relative to properties of thirteen different soils. *Science of the Total Environment*, *511*, 435–443. https://doi.org/10.1016/j.scitotenv.2014.12.088

Kodešová, R., Klement, A., Golovko, O., Fér, M., Kočárek, M., Nikodem, A., & Grabic, R. (2019a). Soil influences on uptake and transfer of pharmaceuticals from sewage sludge amended soils to spinach. *Journal of Environmental Economics and Management*, *250*, 109407. https://doi.org/10.1016/J.JENVMAN.2019.109407

Kodešová, R., Klement, A., Golovko, O., Fér, M., Nikodem, A., Kočárek, M., & Grabic, R. (2019b). Root uptake of atenolol, sulfamethoxazole and carbamazepine, and their transformation in three soils and four plants. *Environmental Science and Pollution Research*, *26*(10), 9876–9891. https://doi.org/10.1007/s11356-019-04333-9

Kodešová, R., Kočárek, M., Klement, A., Golovko, O., Koba, O., Fér, M., et al. (2016). An analysis of the dissipation of pharmaceuticals under thirteen different soil conditions. *Science of the Total Environment*, *544*, 369–381. https://doi.org/10.1016/j.scitotenv.2015.11.085

Kumar, K., & Gupta, S. C. (2016). A framework to predict uptake of trace organic compounds by plants. *Journal of Environmental Quality*, *45*(2). https://doi.org/10.2134/jeq2015.06.0261

Lange, C., Schneider, M., Mutz, M., Haustein, M., Halle, M., Seidel, M., et al. (2015). Model-based design for restoration of a small urban river. *Journal of Hydro-environment Research*, *9*(2), 226–236. https://doi.org/10.1016/j.jher.2015.04.003

Larsen, M., Trapp, S., & Pirandello, A. (2004). Removal of cyanide by woody plants. *Chemosphere*, *54*(3), 325–333. https://doi.org/10.1016/S0045-6535(03)00662-3

Legind, C. N., Kennedy, C. M., Rein, A., Snyder, N., & Trapp, S. (2011). Dynamic plant uptake model applied for drip irrigation of an insecticide to pepper fruit plants. *Pest Management Science*, *67*(5), 521–527. https://doi.org/10.1002/ps.2087

Legind, C. N., Rein, A., Serre, J., Brochier, V., Haudin, C. S., Cambier, P., et al. (2012). Simultaneous simulations of uptake in plants and leaching to groundwater of cadmium and lead for arable land amended with compost or farmyard manure. *PLOS One*, *7*(10), e47002. https://doi.org/10.1371/journal.pone.0047002

Li, H., Sheng, G., Chiou, C. T., & Xu, O. (2005). Relation of organic contaminant equilibrium sorption and kinetic uptake in plants. *Environmental Science & Technology*, *39*(13), 4864–4870. https://doi.org/10.1021/es050424z

Malchi, T., Maor, Y., Tadmor, G., Shenker, M., & Chefetz, B. (2014). Irrigation of root vegetables with treated wastewater: Evaluating uptake of pharmaceuticals and the associated human health risks. *Environmental Science & Technology*, *48*(16), 9325–9333. https://doi.org/10.1021/es5017894

Manoli, G., Bonetti, S., Domec, J. C., Putti, M., Katul, G., & Marani, M. (2014). Tree root systems competing for soil moisture in a 3D soil-plant model. *Advances in Water Resources*, *66*, 32–42. https://doi.org/10.1016/j.advwatres.2014.01.006

Manoli, G., Huang, C. W., Bonetti, S., Domec, J. C., Marani, M., & Katul, G. (2017). Competition for light and water in a coupled soil-plant system. *Advances in Water Resources*. https://doi.org/10.1016/j.advwatres.2017.08.004

Mattina, M. I., Lannucci-Berger, W., Musante, C., & White, J. C. (2003). Concurrent plant uptake of heavy metals and persistent organic pollutants from soil. *Environmental Pollution*, *124*(3), 375–378. https://doi.org/10.1016/s0269-7491(03)00060-5

Morris, M. D. (1991). Factorial sampling plans for preliminary computational experiments. *Technometrics*, *33*(2), 161–174. https://doi.org/10.2307/1269043

Nolan, B. T., Randal Bayless, E., Green, C. T., Garg, S., Voss, F. D., Lampe, D. C., et al. (2005). *Evaluation of unsaturated-zone solute-transport models for studies of agricultural chemicals*. Reston, VA: U.S. Geological Survey.

Ouyang, Y. (2002). Phytoremediation: Modeling plant uptake and contaminant transport in the soil-plant-atmosphere continuum. *Journal of Hydrology*, *266*(1-2), 66–82. https://doi.org/10.1016/S0022-1694(02)00116-6

Peters, A., & Durner, W. (2008). Simplified evaporation method for determining soil hydraulic properties. *Journal of Hydrology*, *356*(1-2), 147–162. https://doi.org/10.1016/j.jhydrol.2008.04.016

Rein, A., Legind, C. N., & Trapp, S. (2011). New concepts for dynamic plant uptake models. *SAR QSAR Environment Research*, *22*(1-2), 191–215. https://doi.org/10.1080/1062936X.2010.548829

Ritchie, J. T. (1972). Model for predicting evaporation from a row crop with incomplete cover. *Water Resources Research*, *8*(5), 1204–1213. https://doi.org/10.1029/WR008i005p01204

Ryan, J. A., Bell, R. M., Davidson, J. M., & O'Connor, G. A. (1988). Plant uptake of non-ionic organic chemicals from soils. *Chemosphere*, *17*(12), 2299–2323. https://doi.org/10.1016/0045-6535(88)90142-7

Sabourin, L., Duenk, P., Bonte-Gelok, S., Payne, M., Lapen, D. R., & Topp, E. (2012). Uptake of pharmaceuticals, hormones and parabens into vegetables grown in soil fertilized with municipal biosolids. *Science of the Total Environment*, *431*, 233–236. https://doi.org/10.1016/j.scitotenv.2012.05.017

Saltelli, A., & Annoni, P. (2010). How to avoid a perfunctory sensitivity analysis. *Environmental Modelling & Software*, *25*(12), 1508–1517. https://doi.org/10.1016/j.envsoft.2010.04.012

Sandermann, H. (1992). Plant metabolism of xenobiotics. *Trends in Biochemical Sciences*, *17*(2), 82–84. https://doi.org/10.1016/0968-0004(92)90507-6

Sandermann, H. (1994). Higher plant metabolism of xenobiotics: The 'green liver' concept. *Pharmacogenetics*, *4*(5), 225–241. https://doi.org/10.1097/00008571-199410000-00001

Scanlon, B. R., Christman, M., Reedy, R. C., Porro, I., Simunek, J., & Flerchinger, G. N. (2003). Intercode comparisons for simulating water balance of surficial sediments in semiarid regions. *Water Resources Research*, *38*(12), WR001233. https://doi.org/10.1029/2001wr001233

Scanlon, B. R., Keese, K., Reedy, R. C., Simunek, J., & Andraski, B. J. (2003). Variations in flow and transport in thick desert vadose zones in response to paleoclimatic forcing (0-90 kyr): Field measurements, modeling, and uncertainties. *Water Resources Research*, *39*(7), WR001604. https://doi.org/10.1029/2002WR001604

Schaap, M. G., Leij, F. J., & Van Genuchten, M. T. (2001). Rosetta: A computer program for estimating soil hydraulic parameters with hierarchical pedotransfer functions. *Journal of Hydrology*, *251*(3-4), 163–176. https://doi.org/10.1016/S0022-1694(01)00466-8

Schroeder, P. R.Aziz, N. M., Lloyd, C. M., & Zappi, P. A. (1994). *The Hydrologic Evaluation of Landfill Performance (HELP) Model:User's Guide for Version 3, EPA/600/R-94/168a*. Washington, DC: U.S. Environmental Protection Agency Office of Research and Development.

Shelia, V., Šimunek, J., Boote, K., & Hoogenbooom, G. (2018). Coupling DSSAT and HYDRUS-1D for simulations of soil water dynamics in the soil-plant-atmosphere system. *Journal of Hydrology Hydromechanics*, *66*(2), 232–245. https://doi.org/10.1515/johh-2017-0055

Šimůnek, J., & Hopmans, J. W. (2009). Modeling compensated root water and nutrient uptake. *Ecological Modelling*, *220*(4), 505–521. https://doi.org/10.1016/j.ecolmodel.2008.11.004

Šimůnek, J., van Genuchten, M. T., & Šejna, M. (2016). Recent developments and applications of the HYDRUS computer software packages. *Vadose Zone Journal*, *15*(7). https://doi.org/10.2136/vzj2016.04.0033

So, E. L., Ruggles, K. H., Cascino, G. D., Ahmann, P. A., & Weatherford, K. W. (1994). Seizure exacerbation and status epileptics related to carbamazepine-10,11-epoxide. *Annals of Neurology*, *35*(6), 743–746. https://doi.org/10.1002/ana.410350616

Stroh, M., Hutmacher, M. M., Pang, J., Lutz, R., Magara, H., & Stone, J. (2013). Simultaneous pharmacokinetic model for rolofylline and both M1-trans and M1-cis metabolites. *The AAPS Journal*, *15*(2), 498–504. https://doi.org/10.1208/s12248-012-9443-5

Sutanto, S. J., Wenninger, J., Coenders-Gerrits, A. M. J., & Uhlenbrook, S. (2012). Partitioning of evaporation into transpiration, soil evaporation and interception: A comparison between isotope measurements and a HYDRUS-1D model. *Hydrology and Earth System Sciences*, *16*(8), 2605–2616. https://doi.org/10.5194/hess-16-2605-2012

Taylor, S. A., & Ashcroft, G. L. (1972). *Physical edaphology: The physics of irrigated and nonirrigated soils*. San Francisco: W.H. Freeman.

Thompson, N. (1983). Diffusion and uptake of chemical vapour volatilising from a sprayed target area. *Pesticide Science*, *14*(1), 33–39. https://doi.org/10.1002/ps.2780140106

Topp, E., Scheunert, I., Attar, A., & Korte, F. (1986). Factors affecting the uptake of 14C-labeled organic chemicals by plants from soil. *Ecotoxicology and Environmental Safety*, *11*(2), 219–228. https://doi.org/10.1016/0147-6513(86)90066-7

Trapp, S. (2007). Fruit tree model for uptake of organic compounds from soil and air. *SAR and QSAR in Environmental Research*, *18*(3-4), 367–387. https://doi.org/10.1080/10629360701303693

Trapp, S. (2009). Bioaccumulation of polar and ionizable compounds in plants. In J. Devillers (Ed.), *Ecotoxicology modeling*. Emerging topics in ecotoxicology (Principles, approaches and perspectives), Vol, (Vol. 2, pp. 299–353). Boston, MA: Springer. https://doi.org/10.1007/978-1-4419-0197-2_11

Trapp, S. (2015). Calibration of a plant uptake model with plant- and site-specific data for uptake of chlorinated organic compounds into radish. *Environmental Science & Technology*, *49*(1), 395–402. https://doi.org/10.1021/es503437p

Trapp, S., & Eggen, T. (2013). Simulation of the plant uptake of organophosphates and other emerging pollutants for greenhouse experiments and field conditions. *Environmental Science and Pollution Research*, *20*(6), 4018–4029. https://doi.org/10.1007/s11356-012-1337-7

Trapp, S., Feificova, D., Rasmussen, N. F., & Bauer-Gottwein, P. (2008). Plant uptake of NaCl in relation to enzyme kinetics and toxic effects. *Environmental and Experimental Botany*, *64*(1), 1–7. https://doi.org/10.1016/j.envexpbot.2008.05.001

Trapp, S., & Matthies, M. (1998). *Chemodynamics and environmental modeling, chemodynamics and environmental modeling: An introduction*. Berlin, Heidelberg: Springer Berlin Heidelberg. https://doi.org/10.1007/978-3-642-80429-8

Travis, C. C., & Arms, A. D. (1988). Bioconcentration of organics in beef, milk, and vegetation. *Environmental Science & Technology*, *22*(3), 271–274. https://doi.org/10.1021/es00168a005

Twarakavi, N. K. C., Sakai, M., & Šimůnek, J. (2009). An objective analysis of the dynamic nature of field capacity. *Water Resources Research*, *45*(10), W10410. https://doi.org/10.1029/2009WR007944

van Genuchten, M. T. (1980). A closed-form equation for predicting the hydraulic conductivity of unsaturated soils1. *Soil Science Society of America Journal*, *44*(5), 892–898. https://doi.org/10.2136/sssaj1980.03615995004400050002x

Vereecken, H., Schnepf, A., Hopmans, J.W., Javaux, M., Or, D., Roose, T., et al., 2016. Modeling soil processes: Review, key challenges, and new perspectives. *Vadose Zone Journal* https://doi.org/10.2136/vzj2015.09.0131, *15*, 5

Vogel, T., Votrubova, J., Dohnal, M., & Dusek, J. (2017). A simple representation of plant water storage effects in coupled soil water flow and transpiration stream modeling. *Vadose Zone Journal*, *16*(5). https://doi.org/10.2136/vzj2016.12.0128

Warner, T., Patsalos, P.N., Prevett, M., Elyas, A.A., Duncan, J.S., 1992. Lamotrigine-induced carbamazepine toxicity: An interaction with carbamazepine-10,11-epoxide. *Epilepsy Research* https://doi.org/10.1016/0920-1211(92)90049-Y

Wen, B., Wu, Y., Zhang, H., Liu, Y., Hu, X., Huang, H., & Zhang, S. (2016). The roles of protein and lipid in the accumulation and distribution of perfluorooctane sulfonate (PFOS) and perfluorooctanoate (PFOA) in plants grown in biosolids-amended soils. *Environmental Pollution*, *216*, 682–688. https://doi.org/10.1016/j.envpol.2016.06.032

Werner, C., & Dubbert, M. (2016). Resolving rapid dynamics of soil-plant-atmosphere interactions. *New Phytologist*, *210*(3), 767–769. https://doi.org/10.1111/nph.13936

Wesseling, J., Elbers, J., Kabat, P., Van den Broek, B. , 1991. SWATRE: Instructions for input. Intern. Note, Winand Star. Cent.

Yang, J., Yu, Q., & Gong, P. (2008). Quantifying air pollution removal by green roofs in Chicago. *Atmospheric Environment*, *42*(31), 7266–7273. https://doi.org/10.1016/j.atmosenv.2008.07.003

Yu, X., Trapp, S., Zhou, P., Wang, C., & Zhou, X. (2004). Metabolism of cyanide by Chinese vegetation. *Chemosphere*, *56*(2), 121–126. https://doi.org/10.1016/j.chemosphere.2004.02.008

Zeng, C. Z., Bie, Z. L., & Yuan, B. Z. (2009). Determination of optimum irrigation water amount for drip-irrigated muskmelon (Cucumis melo L.) in plastic greenhouse. *Agricultural Water Management*, *96*(4), 595–602. https://doi.org/10.1016/j.agwat.2008.09.019

Zhang, H., Chen, J., Ni, Y., Zhang, Q., & Zhao, L. (2009). Uptake by roots and translocation to shoots of polychlorinated dibenzo-p-dioxins and dibenzofurans in typical crop plants. *Chemosphere*, *76*(6), 740–746. https://doi.org/10.1016/j.chemosphere.2009.05.030